Agenzia Nazionale per le Nuove Tecnologie,
l'Energia e lo Sviluppo Economico Sostenibile

Ministero dello Sviluppo Economico

RICERCA DI SISTEMA ELETTRICO

Experimental investigation of thermal hydraulic instabilities in Steam Generator helical coil tubes

M. Colombo, D. Papini, A. Cammi, M.E. Ricotti

Report RdS/2011/105

EXPERIMENTAL INVESTIGATION OF THERMAL HYDRAULIC INSTABILITIES IN STEAM GENERATOR HELICAL COIL TUBES

M. Colombo, D. Papini, A. Cammi, M.E. Ricotti - POLIMI

Settembre 2011

Report Ricerca di Sistema Elettrico
Accordo di Programma Ministero dello Sviluppo Economico – ENEA
Area: Governo, Gestione e sviluppo del sistema elettrico nazionale
Progetto: Nuovo nucleare da fissione: collaborazioni internazionali e sviluppo competenze in materia nucleare

Responsabile Progetto: Paride Meloni, ENEA

CIRTEN

Consorzio **I**nteruniversitario per la **R**icerca **TE**cnologica **N**ucleare

POLITECNICO DI MILANO

DIPARTIMENTO DI ENERGIA, Sezione INGEGNERIA NUCLEARE-CeSNEF

Experimental investigation of thermal hydraulic instabilities in Steam Generator helical coil tubes

M. Colombo, D. Papini, A. Cammi, M.E. Ricotti

CERSE POLIMI RL 1355/2011

Milano, Settembre 2011

Lavoro svolto in esecuzione della linea progettuale LP2– punto B2b
AdP MSE - ENEA "Ricerca di Sistema Elettrico" - PAR2008-09
Progetto 1.3 – "Nuovo Nucleare da Fissione".

INDEX

EXECUTIVE SUMMARY

This document presents the research activities carried out by Politecnico di Milano on the subject of Density Wave Oscillations (DWOs), probably the most representative instabilities encountered in boiling systems. DWOs may constitute an issue of special interest for all the industrial systems and equipments operating with water-steam mixture. Concerning the nuclear field, instability phenomena can be triggered both in Boiling Water Reactor (BWR) fuel channels (where they are moreover coupled through neutronic feedbacks with the neutron field) and in once-through steam generators (SGs), which experience boiling phenomena inside parallel tubes. The latter, in particular, are considered in this document with respect to integral Small-medium Modular Reactor (SMR) applications.

In steam power systems extensive attention is required to avoid thermal induced oscillations of the flow rate and system pressure, as they can cause mechanical vibrations, problem of system control and heat transfer surface burn-out issues. In addition, instability becomes very difficult to be detected in presence of parallel channels, since the total mass flow rate in the system remains constant while the instability is locally triggered among some of the channels. In this conditions, continual cycling of the wall temperature can lead to thermal fatigue problems which may result in tube failure. As a consequence the importance of determining the safe operating regions of a steam generator through definition of the threshold values of system parameters such as flow rate, pressure, inlet temperature and exit quality. To the aim, both basic experiments and numerical analyses are necessary.

The Nuclear Engineering Division of the Department of Energy carried out an extensive research program, both experimental and theoretical, focused on DWOs in parallel channels, in particular dealing with two helically coiled tubes of the IRIS (International Reactor Innovative and Secure) steam generator [1]. *The experimental activity presented the unique feature to investigate the influence of the helical shape (through the centrifugal field induced by tube bending) on instability occurrence, as well as to provide a useful database for models validation and numerical codes assessment. Together with experiments, the development of dedicated analytical models and the adoption of proper numerical simulation tools was of utmost importance to prepare the campaign (pre-test analysis) and interpret the data collected (post-test analysis), gaining an insight into the physical mechanism at the source of DWOs. Main achievements of the research activity are collected in this report.*

The experimental program was realized in a full-scale open loop test facility installed and operated at SIET labs in Piacenza, simulating the thermal hydraulic behaviour of a helically coiled SG [2]. *The facility includes two helical tubes representing the SG of an integral Pressurized Water Reactor (PWR) of Generation III+, connected via lower and upper headers. Experiments were conducted at 3 different levels of pressure (80 bar, 40 bar and 20 bar) and 3 values of mass flux (600 kg/m^{2}s,400 kg/m^{2}s and 200 kg/m^{2}s), exploring a large range of inlet subcoolings between -30% and the saturation value. The test matrix was executed maintaining fixed the configuration of inlet valves (corresponding valve loss coefficient k_{in} = 45). The effect of inlet throttling was at last studied at 40 bar and 400 kg/m^{2}s.*

Data collected permitted to underline many distinctive features of DWOs and to characterize the stable and unstable operating regions of the system, so the effects of system pressure, flow rate and inlet subcooling on the power at the onset of instability. While the effects of thermal power and mass flow rate in determining the channel exit quality triggering the instability was found consistent with classical DWO theory in straight channels, experimental data highlighted a peculiar effect of inlet subcooling. In particular, an increase in inlet subcooling is known from literature to have a stabilizing effect at high subcoolings and a destabilizing effect at low subcoolings. Conversely, in accordance

with experimental data, at low subcoolings the subcooling maintains its stabilizing effect, which increases indeed as the inlet temperature approaches the saturation value. Discrepancies were found also in the values of the period to transit time ratio. In particular the period of oscillations appears rather independent on inlet subcooling and causes the period to transit time ratio to increase with the inlet temperature. Mentioned deviations from literature results have been ascribed to the helical geometry and the peculiar geometrical characteristics of the test section.
Finally, some Ledinegg-type instabilities have been recorded in particular operating conditions, that is at the lowest system pressure (p = 20 bar), the highest mass flux (G = 600 kg/m^{2}s) and higher inlet subcooling values (x_{in} < -15%). Therefore they are briefly discussed and analysed in this report.

The modelling effort was mainly focused on the development of an analytical lumped parameter model, moving boundary type, based on the integration of mass, energy and momentum 1D equations. Homogeneous two-phase flow model has been assumed in the boiling region. Non-linear features of the modelling equations permitted to investigate the complex phenomena and interactions being at the source of the instability mechanism. Moreover several sensitivity studies were made to identify in the proper simulation of two-phase frictional pressure drop the most critical issue for a correct prediction of the instability threshold.
The analytical model was applied at first to the simple and acknowledged case of vertical tube geometry and the theoretical predictions have been validated with qualified numerical simulation tools. Both the thermal hydraulic code RELAP5 and the multi-physics code COMSOL have been successfully applied to predict instability thresholds obtaining a useful validation benchmark for the developed models [3].
As concerns the COMSOL multi-physics code, a thermal hydraulic 1D simulator for water-steam mixture has been developed, including both single-phase and two-phase regions. Initially the simple homogeneous flow model (HEM) was assumed, as for the analytical model, but afterwards also the more accurate Drift-Flux Model (DFM) was implemented. The latter permits to account for slip effects due to the relative velocity between the two-phases.
In addition to the comparison of stability maps obtained with time domain simulations, also a linear stability analysis leading to the definition of system eigenvalues was successfully completed, both with the analytical model and the COMSOL code. Linear analysis showed to be a quick and powerful tool generally for instability studies and in particular when addressing the influence of the two-phase friction model. In this respect, thanks to the possibility of implementing most various kinds of two-phase flow models, the COMSOL code demonstrated the capability to be easily adaptable to many different heated channel systems.
As concerns the RELAP5 code, a preliminary code assessment procedure has been addressed, aiming at highlighting its strengths and weaknesses with respect to DWO predictions. As stated before, instability thresholds were correctly reproduced by the code dealing with simple vertical tube geometry, both in single and in parallel channel configurations [4][5]. *To reproduce the experimental facility installed at SIET labs, 32 m long and 8 m high, inclined tubes have been modelled with the RELAP5 code. A parametric study has been made changing step by step geometric parameters, considering separately channel length and channel inclination. The influence of the inclination was correctly reproduced, resulting in a more stable system when approaching vertical orientation at fixed tube length, due to the increase in gravitational pressure drops. Larger stability region was recorded increasing channel length at fixed inclination in case of two parallel channels, the same effect vanishing instead in single heated channels. The latter result seems to suggest some difficulties of the RELAP5 code in addressing more complex geometry with respect to a simple vertical channel.*

Finally the results provided by the analytical model and the RELAP5 code have been compared to the experimental data for validation purposes. The analytical model has been satisfactorily applied to the simulation of the experimental results. Correct representation of the stationary pressure drop distribution (partially accomplished thanks to the experimental tuning of a sound friction correlation) has been identified as fundamental before providing any accurate instability calculations. In this respect, the RELAP5 code cannot be regarded for the time being as a proven tool to study DWO phenomena in helically coiled tubes.

The activity characterized itself has the prosecution of the project line LP2.G1 of PAR 2007, reported in [6] and focused essentially on pre-test analyses. For the sake of clarity some subjects of [6] are recovered in this report, in particular a general presentation on the subject of Density Wave Oscillations in Section 1, the description of the experimental facility, the experimental procedure and the explored variables in Section 2 and a brief presentation of the analytical model development in Section 3. Preliminary limited experimental and analytical model results already included in [6] are also repeated.

1 DENSITY WAVE OSCILLATIONS

1.1 Introductory background on density wave instability

Density Wave Oscillations (DWOs) and more generally two-phase flow instabilities have been studied since the '60, being of interest to the design and operation of many different industrial systems. As a matter of fact, thermally induced oscillations of the flow rate and system pressure are undesirable, as they can cause mechanical vibrations, thermal fatigue, problems of system control, and in extreme circumstances disturb the heat transfer and promote thermal crisis occurrence. Thus, it is of great importance to study the effect on the onset of instability of system parameters such as thermal power, flow rate, pressure, inlet temperature and exit quality. The evaluation of the instability threshold values permits to determine the safe operating regions of a two-phase heat exchanger.

The various types of self-sustained oscillations which could arise in a boiling channel have been reviewed and classified in different literature works [6][8][9]. Density Wave Oscillations (DWOs) are classified among "dynamic type" instabilities, as they are triggered by transient inertia, lags and feedbacks between the flow rate, the vapor generation rate and the pressure drops in the boiling channel. A description of the physical mechanism leading to the appearance of DWOs is provided by Yadigaroglu and Bergles [10], with respect to a single heated channel with an imposed total pressure drop across. DWOs are induced by delays in the transient distribution of pressure drops along the tube, which originate from the difference in density between the subcooled liquid entering the channel and the water-steam mixture exiting. If the pressure drop along the channel is imposed, a sudden pressure drop perturbation necessarily leads to a flow rate perturbation. An instantaneous perturbation of the flow rate causes an enthalpy perturbation propagating throughout the channel, which affects both the boiling boundary position and the length of the single-phase and two-phase regions. The result is a perturbation in the single-phase pressure drop - say $\delta\Delta p_1$ - and a delayed two-phase pressure drop perturbation of the opposite sign - say $\delta\Delta p_2$ -. The latter creates a feedback pressure perturbation of the opposite sign in the single-phase region, which can either attenuate or reinforce $\delta\Delta p_1$. With correct timing, single-phase region and two-phase region pressure terms oscillate in counter-phase, flow oscillation becomes self-sustained and waves of "heavier" (higher density) and "lighter" (lower density) fluid propagate through the channel (Figure 1). According to this description, as an oscillating cycle is completed by the passage of two perturbations, the period of oscillations should be of the order of twice the mixture transit time.

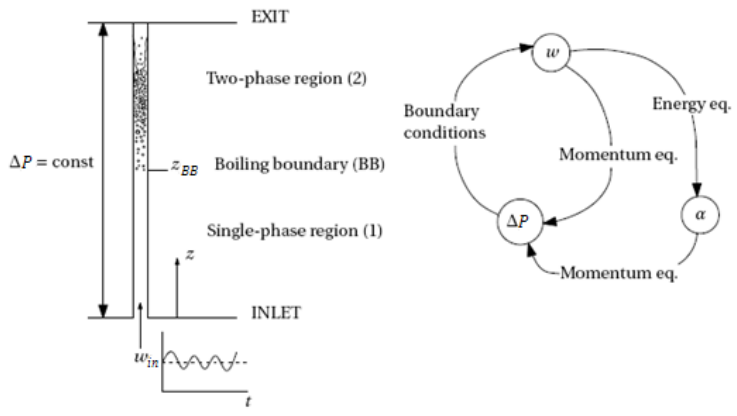

Figure 1 - Density wave instability mechanism in a single boiling channel, and respective feedbacks between main physical quantities. (Reproduced from [7]).

In recent years, Podowski [11] and Rizwan-uddin [12] proposed different descriptions based on more complex relations between the system parameters. Their explanation is based on the different speeds of propagation of velocity perturbations between the single-phase region (speed of sound) and the two-phase region (so named kinematic velocity). The oscillations seem to be more likely related to mixture velocity variations rather than to mixture density variations, in particular at high inlet subcoolings. The result is a period of oscillations equal to even three or four times the mixture transit time.

The operating point of a boiling channel is therefore determined by many different parameters, which also influence its stability. Once fluid properties, channel geometry and system operating pressure have been defined, major role is played by the three quantities flow rate Γ, inlet subcooling Δh_{in} (in enthalpy units) and total thermal power q supplied to the channel. Therefore stable and unstable system operating regions could be represented in a three-dimensional space (Γ, Δh_{in}, q), whereas a mapping of these regions in two dimensions is referred to as the stability map of the system. No universal stability map exists, and different ones have been proposed over the years. The most successful is due to Ishii and Zuber [13], who introduced phase change number N_{pch} and subcooling number N_{sub}. The phase change number scales the characteristic frequency of phase change Ω to the inverse of a single-phase transit time in the system, instead the subcooling number measures the inlet subcooling:

$$N_{pch} = \frac{\Omega}{w_{in}/L} = \frac{\frac{v_{lv}\cdot q'''}{h_{lv}}}{w_{in}/L} = \frac{q}{\Gamma\cdot h_{lv}}\cdot\frac{v_{lv}}{v_l}; \tag{1}$$

$$N_{sub} = \frac{\Delta h_{in}}{h_{lv}}\cdot\frac{v_{lv}}{v_l}. \tag{2}$$

The advantage of Ishii's dimensionless parameters is that they include the effect of pressure variations through the ratio between specific volumes (v_{lv}/v_l). A typical stability map in the N_{pch}-N_{sub} plane is depicted in Figure 2. The usual stability boundary shows the classical "L shape" inclination and follows a line of nearly constant equilibrium quality at high inlet subcooling. The stability boundary divides the N_{pch}-N_{sub} space in two regions: the stable region on the left-hand side (lower N_{pch}, lower power supplied) and the unstable region on the right-hand side (higher N_{pch}, higher power supplied).

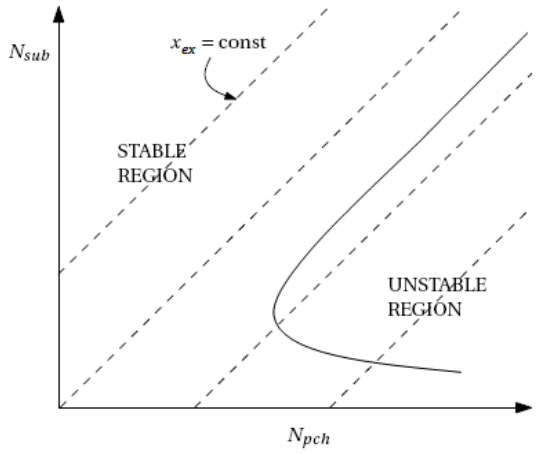

Figure 2 – Example of stability map in the dimensionless plane N_{pch} - N_{sub}.

Figure 2 allows identifying the effect of different parameters on the system stability.

Effect of thermal power, flow rate and exit quality. An increase in thermal power supplied to the channel is destabilizing. In the same way, a stable system can be made unstable reducing the flow rate. Both effects increase the exit quality, which turns out to be a key parameter for system stability. The destabilizing effect of increasing the ratio q/Γ is universally accepted.

Effect of inlet subcooling. The effect of inlet subcooling increase is stabilizing at high subcoolings and destabilizing at low subcoolings. Instability threshold assumes therefore the classical "L shape". This behavior is explainable by the fact that an increase or a decrease of inlet subcooling shifts the channel toward single-phase liquid and vapor operation respectively, hence out of the unstable two-phase operating mode.

Effect of pressure level. An increase in operating pressure is found to be stabilizing, although one must be careful in stating which system parameters were kept constant while the pressure level was increased. Ishii [14] showed that stability boundaries calculated at three different pressure levels were almost overlapped in the N_{pch}-N_{sub} plane, demonstrating the usefulness of v_{lv}/v_l ratio adopted in the dimensionless numbers to account for pressure effect.

Effect of inlet and exit throttling. The effect of inlet throttling is always strongly stabilizing, leading to an increase of single-phase pressure drop term, which promotes system stability. A flow resistance is frequently placed at channel inlet to assure stability of otherwise unstable channel. On the contrary, exit throttling is found to be destabilizing, by increasing two-phase region pressure drops, which act against system stability.

1.2 Review of density wave instability studies

1.2.1 Experimental investigations on density wave oscillations

The majority of the experimental works on the subject, collected in several literature reviews [6][9], deals with straight tubes and few meters long test sections. Moreover, all the aspects associated with DWO instability have been systematically analysed in a limited number of works. Systematic study of density wave instability means to produce well controlled experimental data on the onset and the frequency of this type of oscillation, at various system conditions (and with various operating fluids).

Amongst them, are worthy of mention the pioneering experimental works of Saha et al. [15], using a uniformly heated single boiling channel with bypass, and of Masini et al. [16], working with two vertical parallel tubes. To the best of our knowledge, scarce number of experiments was conducted studying full-scale long test sections (with steam generator tubes application), and no data are available on the helically coiled tube geometry (final objective of the present work). Indeed, numerous experimental campaigns were conducted in the past using refrigerant fluids (such as R-11, R-113 ...), due to the low critical pressure, low boiling point, and low latent heat of vaporization. That is, for instance, the case of the utmost work of Saha et al. [15], where R-113 was used as operating fluid.

In the recent years, some Chinese researches [17] experimentally studied the flow instability behaviour of a twin-channel system, using water as working fluid. Indeed, a small test section with limited pressure level (maximum pressure investigated is 3 MPa) was considered; systematic execution of a precise test matrix, as well as discussions about the oscillation period, are lacking.

1.2.2 Theoretical researches on density wave oscillations

Two general approaches are possible for theoretical stability analyses on a boiling channel:

- frequency domain, linearized models;
- time domain, non-linear models.

In frequency domain [18], governing equations and necessary constitutive laws are linearized about an operating point and then Laplace-transformed. The transfer functions obtained in this manner are used to evaluate the system stability by means of classic control-theory techniques. This method is inexpensive with respect to computer time, relatively straightforward to implement, and is free of the numerical stability problems of finite difference methods.

The models built in time domain permit either 0D analyses [19][20], based on the analytical integration of conservation equations in the competing regions, or more complex but accurate 1D analyses [21][22][23], by applying numerical solution techniques (finite differences, finite volumes or finite elements). In these models the steady-state is perturbed with small stepwise changes of some operating parameter simulating an actual transient, such as power increase in a real system. The stability threshold is reached when undamped or diverging oscillations are induced. Non-linear features of the governing equations permit to grasp the feedbacks and the mutual interactions between variables triggering a self-sustained density wave oscillation. Time domain techniques are indeed rather time consuming when used for stability analyses, since a large number of cases must be run to produce a stability map, and each run is itself time consuming because of the limits on the allowable time step.

Numerous lumped parameter and distributed parameter stability models, both linear and non-linear, have been published since the '60-'70s. Most important literature reviews on the subject [6][8][9] collect the large amount of theoretical researches. It is just noticed that the study on density wave instabilities in parallel twin or multi-channel systems represents still nowadays a topical research area. For instance, Muñoz-Cobo et al. [19] applied a non-linear 0D model to the study of out-of-phase oscillations between parallel subchannels of BWR cores. In the framework of the future development of nuclear power plants in China, Guo Yun et al. [22] and Zhang et al. [23] investigated DWO instability in parallel multi-channel systems by using control volume integrating method. Schlichting et al. [20] analysed the interaction of PDOs (Pressure Drop Oscillations) and DWOs for a typical NASA type phase change system for space exploration applications.

1.2.3 Numerical code simulations on density wave oscillations

On the other hands, qualified numerical simulation tools can be successfully applied to the study of boiling channel instabilities, as accurate quantitative predictions can be provided by using simple and straightforward nodalizations.

In this frame, the best-estimate system code RELAP5, based on a six equations non-homogeneous non-equilibrium model for the two-phase systems, was designed for the analysis of all transients and postulated accidents in LWR nuclear reactors, including Loss Of Coolant Accidents (LOCAs) as well as all different types of operational transients [24]. In the recent years, several numerical studies published on DWOs featured the RELAP5 code as the main analysis tool. Amongst them, Ambrosini & Ferreri [25] performed a detailed analysis about thermal hydraulic instabilities in a boiling channel using the RELAP5/MOD3.2 code. In order to respect the imposed constant pressure drop boundary condition, which is the proper boundary condition to excite the dynamic feedbacks that are at the source of the instability mechanism, a single channel layout with impressed pressures, kept constant by two inlet and outlet plena,

was investigated. The Authors demonstrated the capability of the RELAP5 system code to detect the onset of DWO instability.

The multi-purpose COMSOL Multiphysics® numerical code [26] can be applied to study the stability characteristics of boiling systems too. Widespread utilization of COMSOL code relies on the possibility to solve different numerical problems by implementing directly the systems of equations in PDE (Partial Differential Equation) form. Respective PDEs are then solved numerically by means of finite element techniques. It is just mentioned that this approach is globally different from previous one discussed (i.e., the RELAP5 code), which indeed considers finite volume discretizations of the governing equations, and of course from the simple analytical treatments described in Section 3.1. In this respect, linear and non-linear stability analyses by means of the COMSOL code have been provided by Schlichting et al. [27], who developed a 1D drift-flux model applied to instability studies on a boiling loop for space applications.

2 EXPERIMENTAL CAMPAIGN

2.1 The experimental facility

The experimental facility, built and operated at SIET labs, is an extension of an electrically heated test section used for the study of the thermal hydraulics of a helically coiled SG tube (two-phase pressure drops under diabatic and adiabatic conditions and dryout thermal crisis occurrence) [28]. In the framework of the IRIS (International Reactor Innovative and Secure) project [29], the same test section was also included in a closed loop circuit, to study a passive heat removal system with natural circulation [30]. The facility, provided with SG full elevation and suited for prototypical thermal hydraulic conditions reproduction, implements the common simplification given by a constant heat flux boundary (via electrical power) instead of real controlled temperature boundary. When dealing with experiments on instability phenomena, despite different dynamic responses, such different boundary is expected to secondarily affect the instability threshold (as the instability inception is induced by the specific thermal power supplied, owing to the reached thermodynamic quality).

Coil diameter (1 m) has been chosen as representative of a mean value of IRIS steam generator tube, while tube inner diameter (12.53 mm) is the commercially scheduled value nearer to IRIS real value (13.24 mm). The heated tube is thermally insulated by means of rock wool. Thermal losses were measured via runs with single-phase hot pressurized water flowing inside the steam generator, and estimated as a function of the temperature difference between external tube wall and the environment.

The facility was renewed to test DWOs in parallel channels, by adding a second helical tube identical to the first one (same coil diameter, pitch and length). The two helices have been connected with common lower and upper headers to provide the constant pressure drop boundary condition required for the instability inception. The conceptual sketch of the new facility is depicted in Figure 3, whereas a global and a detailed views are provided in Figure 4. Geometrical data of the two helical tubes are listed in Table 1.

The whole facility is made by a supply section and a test section. The supply section feeds demineralized water from a tank to the test section, by means of a centrifugal booster pump and a feed water pump, i.e. a volumetric three cylindrical pump with a maximum head of about 200 bar.

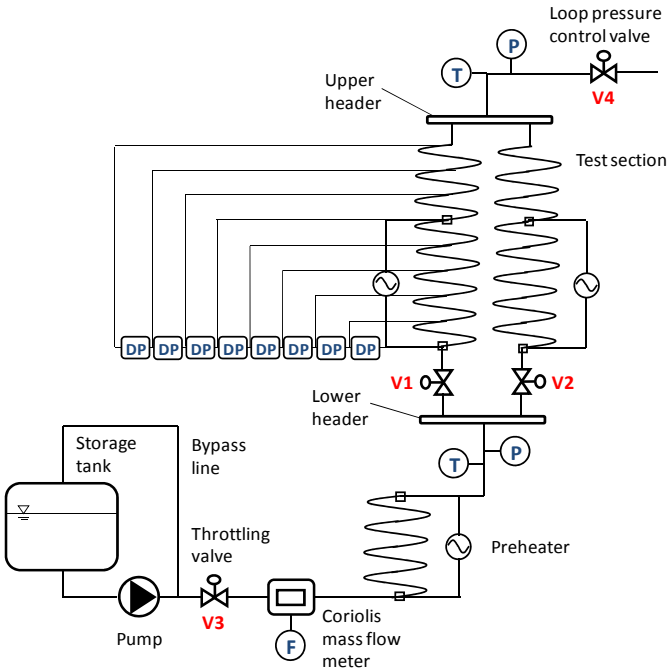

Figure 3 – Sketch of the experimental facility installed at SIET labs.

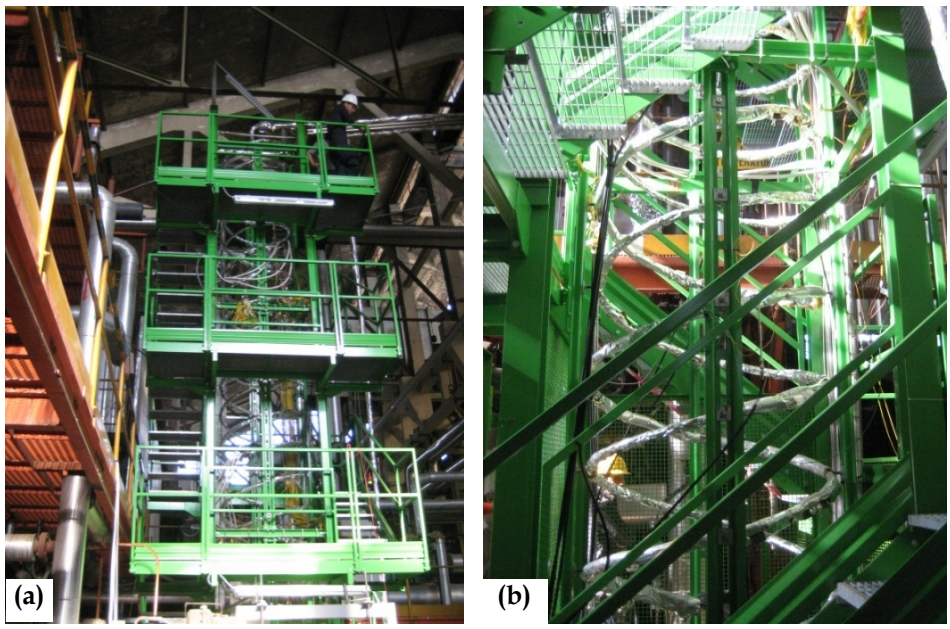

Figure 4 – Global view (a) and detailed picture (b) of the helical coil test facility (SIET labs).

The flow rate is controlled by a throttling valve (V3) positioned downwards the feed water pump and after a bypass line. System pressure control is accomplished by acting on a throttling valve (V4) placed at the end of the steam generator. An electrically heated preheater is located before the test section, and allows creating the desired temperature at the inlet of the test section. The test section is electrically heated via Joule effect by DC current. Two distinct, independently controllable and contiguous sections are provided. For instability experiments, power was supplied only to the first section (24 m), instead the second section (8 m) worked as a riser unheated section.

Table 1 – Test section main data.

Tube material	SS AISI 316L
Tube inner diameter [mm]	12.53
Tube outer diameter [mm]	17.24
Coil diameter [mm]	1000
Coil pitch [mm]	800
Tube length [m]	32
Heated section length [m]	24
Riser length [m]	8
Steam generator height [m]	8

Each tube is provided at inlet with a calibrated orifice (with a differential pressure transmitter) used to measure the flow rate in each channel and to visually detect the instability inception, and with a valve to impose a concentrated pressure drop. V1 and V2 represent the total pressure drop (instrumented orifice + valve) introduced at the inlet of the two helical tubes, respectively.

The water pressures at inlet and outlet headers are measured by absolute pressure transducers; nine pressure taps are disposed nearly every 4 m along one tube and eight differential pressure transducers connect the pressure taps. Detailed distances between the taps are reported in Table 2. An accurate measurement of the total flow rate is obtained by a Coriolis flow-meter, placed between the pump and the preheater. Bulk temperatures are measured with K-class thermocouples drowned in a small well at SG inlet and outlet headers. Wall thermocouples (K-class) are mounted throughout the two coils, with fining near the ends to identify the risk of dryout occurrence. Electrical power is obtained via separate measurement of current (by a shunt) and voltage drop along the test section by a voltmeter.

All the measurement devices have been tested and calibrated at the certified SIET labs. A summary of the uncertainties is reported in Table 3.

Table 2 – Pressure taps distribution along the test section (Channel A).

	Tap 1	Tap 2	Tap 3	Tap 4	Tap 5
Distance from tube inlet [m]	0.20	5.17	9.19	13.15	17.14
	Tap 6	Tap 7	Tap 8	Tap 9	
Distance from tube inlet [m]	21.64	25.59	29.09	32.06	

Table 3 – List of the uncertainties of physical quantities (referred to measurement values).

Water flow rate	± 1%
Fluid bulk and wall temperature	± 0.7 °C
Absolute pressure	± 0.1%
Differential pressure	± 0.4%
Supplied electrical power	± 2.5%
Evaluated thermal losses	± 15%

2.2 Experimental procedure

It was decided to act on the electrical power supplied to the test section in order to reach flow unstable conditions starting from a stable operating system. In every test run, the heating power was gradually increased from nominal values up to the appearance of flow instability.
The adopted test procedure can be summarized in the following steps:

(1) Registration of the gravitational head of the different instruments.
(2) Characterization of the normal behaviour of the system (for instance, check that, at open V1 and V2 valves, the flow rate is reasonably balanced between the two coils).
(3) Impose the defined position of V1 and V2 valves.
(4) Define pressure level.
(5) Impose a value of flow rate.
(6) Impose a value of inlet subcooling by means of the preheater.
(7) Reach the desired pressure level by generating vapour with power increase. When the desired pressure is obtained, keep the system in a steady-state condition (measurements of temperature, pressure, flow rate and heat input).
(8) The electrical power is progressively increased by small amounts (small steps of 2-5 kW per tube), until sustained oscillations are observed (check that the system pressure remains more or less constant).
(9) Once the instability is recorded, take the system back to step 6, and change the subcooling. Repeat steps 7 and 8 up to the instability (same operating pressure).
(10) Once all the subcooling values are tested for a flow rate level, change the flow rate and repeat steps 6-9.
(11) Once all the flow rate values defined in step 5 are completely explored (every subcooling value), change the desired pressure level and repeat steps 5-10.

2.3 Ranges of explored variables

DWOs result from multiple feedback effects between the flow rate, the vapour generation rate and the pressure drops in the boiling channel. To fully describe the stable region of the system and collect information on instability phenomena, it is necessary to determine instability thresholds in a wide range of system operating parameters.
A thorough test matrix was prepared to study the effects of system pressure, mass flow rate and inlet subcooling on system stability, by investigating:

- 3 levels of pressure: 80 bar, 40 bar and 20 bar;
- 3 levels of mass flux: 600 kg/m^{2}s, 400 kg/m^{2}s and 200 kg/m^{2}s;
- several values of inlet subcooling between x_{in} = -30% and x_{in} = 0%.

The entire test matrix was executed with reference to a "basically open" configuration of the inlet valves V1 and V2 (corresponding valve loss coefficient k_{in} = 45). The effect of inlet throttling was at last studied by progressively closing the valves and repeating the stability map at p = 40 bar and G = 400 kg/m^{2}s.

2.4 DWO characterization

DWO appearance in a boiling channel can be detected by monitoring the flow rate, which starts to oscillate when power threshold is reached. The calibrated orifices installed at the inlet of both tubes permit to measure the flow rate through the recording of the pressure drops established across them. Thus, flow instability power threshold was experimentally defined as the power corresponding to permanent and regular flow oscillations, detected by visual observation of the pressure drop recording of the calibrated orifices (within V1 and V2 of Figure 3). The system was considered completely unstable when flow rate oscillation amplitude reached the 100% of its steady-state value. Obviously, flow rate in the two channels oscillates in counter-phase, being the total system mass flow rate imposed, as it is shown in Figure 5, where fully developed DWOs are depicted. The "square wave" shape of the curves is due to the reaching of instruments full scale.

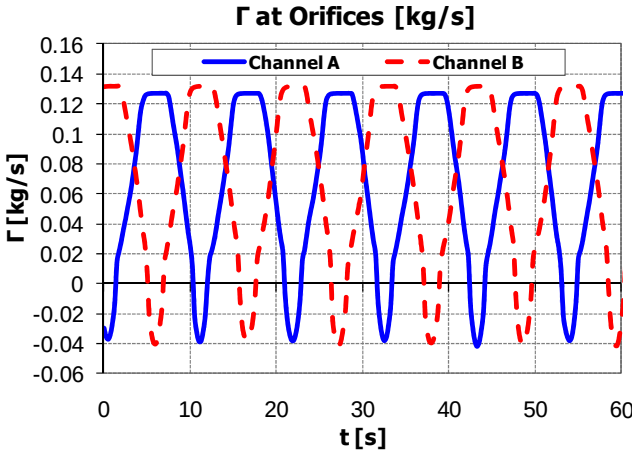

Figure 5 - Flow rate oscillations during fully developed instability. Data collected with: p = 83 bar; T_{in} = 199 °C; G = 597 kg/m^{2}s; q = 99.3 kW.

Data collected during instability inception and fully developed instability allowed understanding the distinctive features of DWOs. System pressure oscillates with a frequency that is double if compared with the frequency of flow rate oscillations (Figure 6). Similar behaviour is exhibited by the total pressure drop, common to both the channels (i.e., the pressure difference between lower header and upper header of the facility). When the system is unstable, it is evident that there are two oscillations of total $\Delta p(t)$ per single oscillation of channel flow rate ("first" oscillation is due to Channel A, and "second" oscillation is due to Channel B, Figure 7).

Counter-phase oscillation of single-phase and two-phase pressure drops within each channel is known to be one of the triggering events leading to the appearance of DWOs. Figure 8 compares the pressure drops between pressure taps placed on different regions of Channel A (according to the distribution depicted in Table 2), in case of self-sustained instability. Pressure drops in the single-phase region (DP 2-3) oscillate in counter-phase with respect to two-phase pressure drops (DP 6-7 and DP 8-9). The phase shift is not abrupt, but it appears gradually along the channel. As a matter of fact, the pressure term DP 4-5 (low-quality two-phase region) shows only a limited phase shift with respect to single-phase zone (DP 2-3). Besides, as indicated by theory [6], single-phase pressure drop is oscillating in phase with the inlet velocity (compare Figure 8, DP 2-3, with Figure 5, blue curve). Progressive phase shift of two-phase pressure drop oscillation is the unleashing cause of DWO occurrence.

Moreover, large amplitude fluctuations in channel wall temperatures, so named "thermal oscillations" [9], always occur (Figure 9), associated with fully developed density wave oscillations that trigger intermittent film boiling conditions.

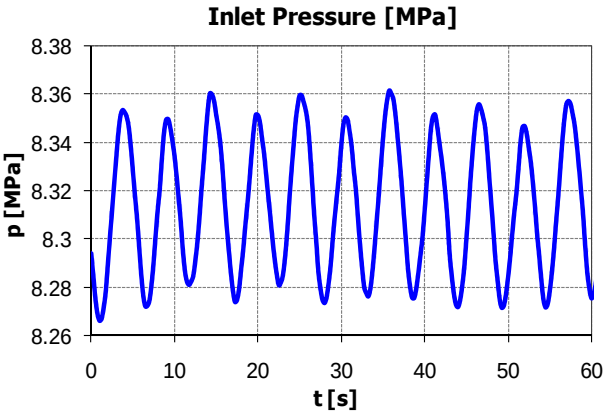

Figure 6 - System pressure oscillations in the inlet header. Data collected with: p = 83 bar; T_{in} = 199 °C; G = 597 kg/m^{2}s; q = 99.3 kW.

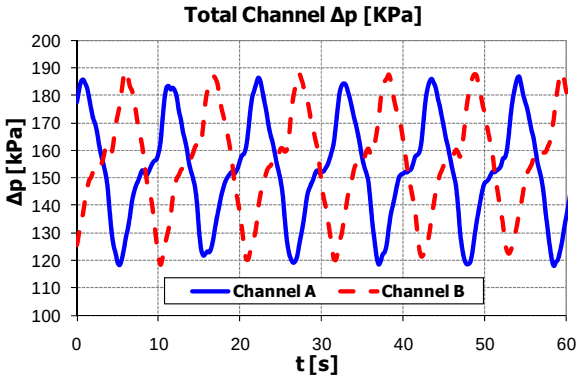

Figure 7 - Counter-phase pressure drop oscillations in the two parallel tubes. Data collected with: p = 83 bar; T_{in} = 199 °C; G = 597 kg/m^{2}s; q = 99.3 kW.

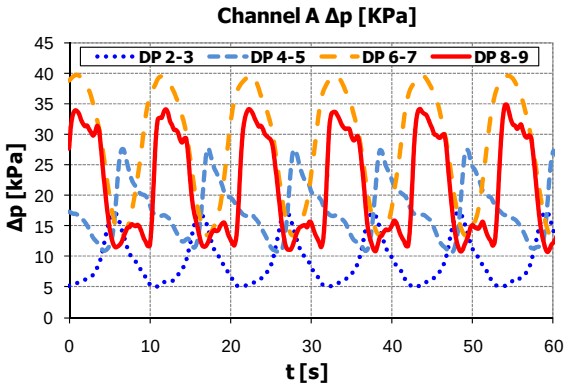

Figure 8 - Pressure drop oscillations in different regions of channel A: single phase (DP 2-3), low quality two-phase (DP 4-5), two-phase (DP 6-7 and DP 8-9). Data collected with: p = 83 bar; T_{in} = 199 °C; G = 597 kg/m^{2}s; q = 99.3 kW.

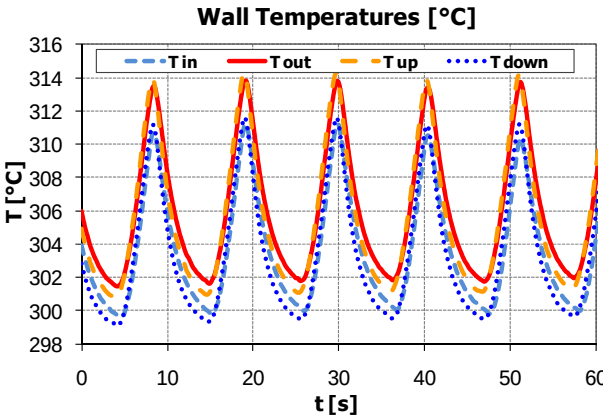

Figure 9 - Fluctuations of tube wall temperatures during DWOs. Data collected with: p = 83 bar; T_{in} = 199 °C; G = 597 kg/m^{2}s; q = 99.3 kW.

2.5 Experimental results

Collected threshold data have been organized on the stability plane N_{pch}-N_{sub}, introduced by Ishii and Zuber [13]. Figure 10, Figure 12 and Figure 14 show the stability maps obtained with the experimental data collected at the three pressure levels investigated in the present helical tubes facility. Error bars have been introduced following uncertainty analysis based on error linear propagation techniques [31]. The uncertainties of final dimensionless numbers within the maps have been computed combining the effects of the various measured quantities.

Main effect is due to threshold power, following the uncertainties of measured electrical power, estimated thermal losses, as well as a term due to the discrete experimental procedure. Effect of pressure is also accounted for, by evaluating the maximum variation between the pressure recorded at instability inception with respect to the nominal pressure level. Pressure term is made apparent by the sensitivity of Eqs. (1), (2) on small pressure variations, which is considerably large at low pressure (such to overcome threshold power uncertainty) [1].

The whole concern was introduced to properly consider different threshold points, collected at slightly different pressures, on a N_{pch}–N_{sub} stability map. In other words, it affects remarkably the results presented at low pressure (20 bar, Figure 12), where the dimensionless numbers are very sensitive to even small variations of the pressure.

The three different curves depicted in each graph represent the instability thresholds for the three values of mass flux (G = 600 kg/m^{2}s, 400 kg/m^{2}s and 200 kg/m^{2}s), testing different inlet subcooling values. At 80 bar only two mass fluxes have been considered, because plant operations resulted difficult at low flow rates. As expected, the stability boundaries according to the various mass flows are almost overlapped. Thus, it is the ratio q/Γ that determines the onset of instability once the characteristics of the channel and the inlet conditions are set. Figure 11, Figure 13 and Figure 15 confirm, for the three pressure levels respectively, that a mass flow rate variation induces a proportional variation of the thermal power needed to trigger the instability. An increase in thermal power or a decrease in channel mass flow rate can cause the onset of DWOs; both effects increase the exit quality, which turns out to be a key parameter for boiling channel instability. In brief, the effects on instability of thermal power and mass flow rate do not show differences in the helical geometry when compared to the straight tube case.

Instead, it is interesting to focus the attention on inlet subcooling. It is well known from literature that an increase in inlet subcooling is stabilizing at high subcoolings and destabilizing at low subcoolings [6]. This behaviour results in the classical "L shape" of the stability boundary, exhibited by all the dimensionless maps available in literature and referred to straight geometry (Figure 2) [13][16][21]. The present datasets with helical geometry confirm the stabilizing effect at high subcoolings. The experimental stability maps show indeed two different behaviours:

- "conventional" at medium-high subcoolings, with iso-quality stability boundary and slight stabilization in the range $N_{sub} = 3 \div 6$ (close to "L shape");
- "non-conventional" at low subcoolings, with marked destabilizing effects as inlet temperature increases and approaches the saturation value.

Such different behaviour exhibited by the stability boundary at low subcoolings can be ascribed to the helical shape of the parallel channels and related centrifugal field effects on the thermal hydraulics of two-phase flow. Also the full-scale length of the test section and the small inclination angle of the helix, affecting two-phase flow pattern, may explain the provided experimental results.

It is just noticed that at the lowest system pressure and lowest mass flux (p = 20 bar and G = 200 kg/m^{2}s, see Figure 12) the stability boundary shape is different from previous discussion and agrees more with classical behaviour given by straight vertical tubes. As a matter of fact, the effect of inlet subcooling increase is stabilizing at high subcoolings, and destabilizing at low subcoolings. The centrifugal field, reasonably weak under these conditions, is such to make the peculiar effect of the helical geometry negligible.

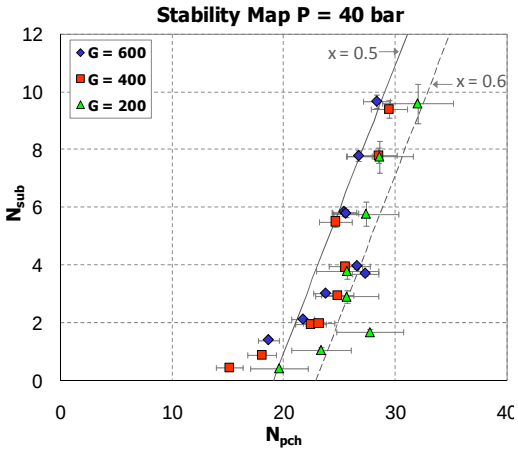

Figure 10 - Stability map obtained at system pressure p = 40 bar and different mass fluxes (G = 600 kg/m^{2}s, 400 kg/m^{2}s, 200 kg/m^{2}s).

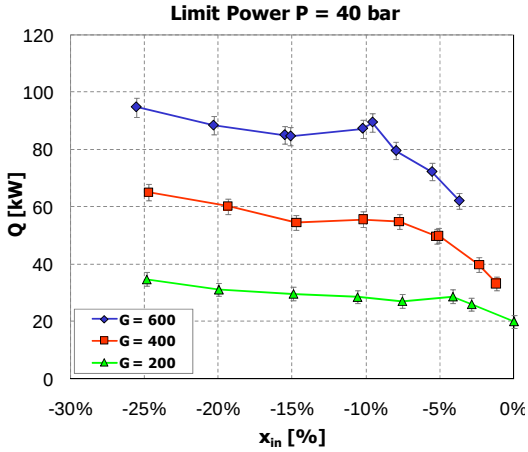

Figure 11 - Limit power for instability inception at p = 40 bar as function of inlet subcooling and for different values of mass flux.

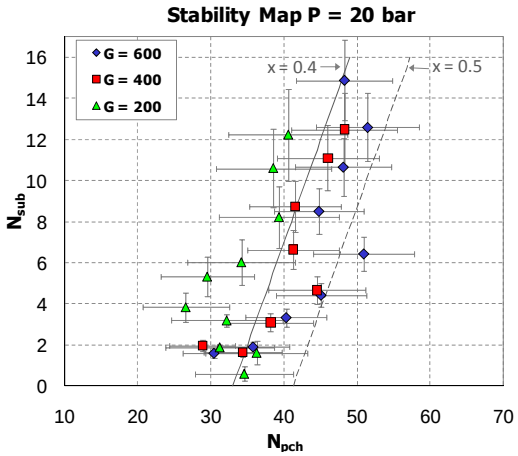

Figure 12 - Stability map obtained at system pressure p = 20 bar and different mass fluxes (G = 600 kg/m^{2}s, 400 kg/m^{2}s, 200 kg/m^{2}s).

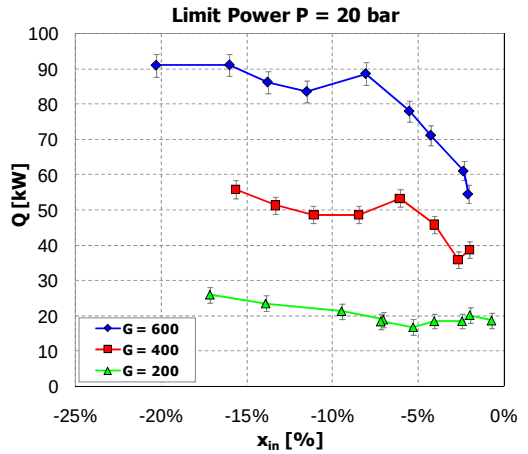

Figure 13 - Limit power for instability inception at p = 20 bar as function of inlet subcooling and for different values of mass flux.

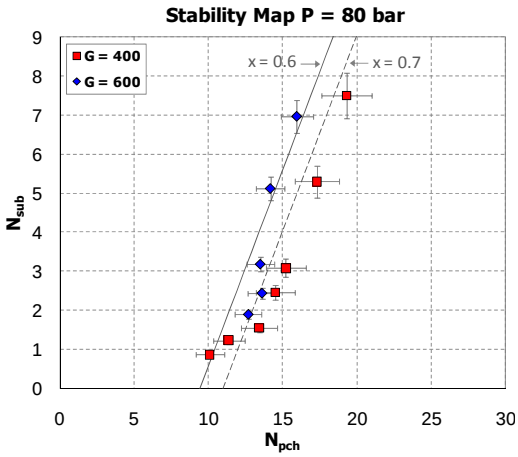

Figure 14 - Stability map obtained at system pressure p = 80 bar and different mass fluxes (G = 600 kg/m^{2}s, 400 kg/m^{2}s).

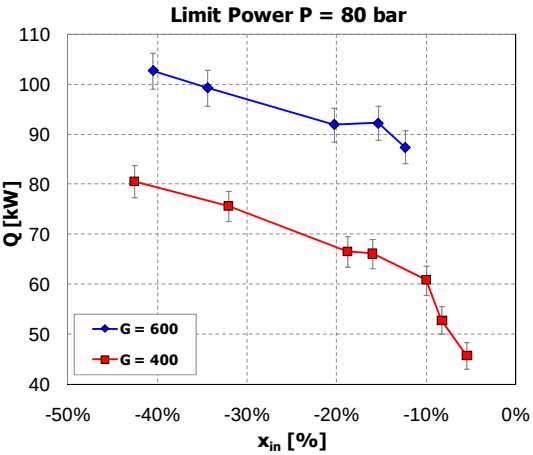

Figure 15 - Limit power for instability inception at p = 80 bar as function of inlet subcooling and for different values of mass flux.

2.5.1 Effect of system pressure

System pressure was always found to be stabilizing, although pressure effect is less effective if compared with other system parameters [6]. Figure 16, Figure 17 and Figure 18 show the limit power corresponding to the various pressure levels, fixed the mass flow rate in the system (G = 200, 400 and 600 kg/m^{2}s respectively). The higher is the pressure, the higher is the exit quality required for the onset of instability, hence the system is more stable. This concern is evident by considering the iso-quality lines reported in the stability maps (Figure 10, Figure 12 and Figure 14). Thermal power behaviour in the figures also confirms the subcooling destabilizing effect for small values of N_{sub}.

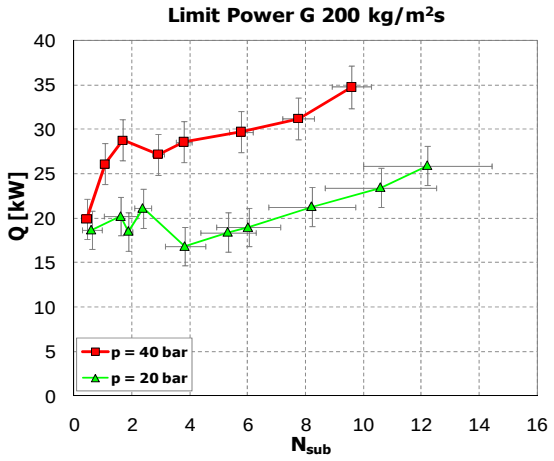

Figure 16 - Limit power for instability inception at G = 200 kg/m^{2}s as function of the subcooling number and at different pressures.

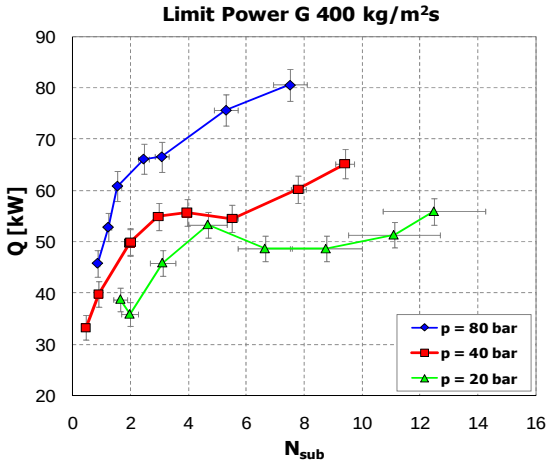

Figure 17 - Limit power for instability inception at G = 400 kg/m^{2}s as function of the subcooling number and at different pressures.

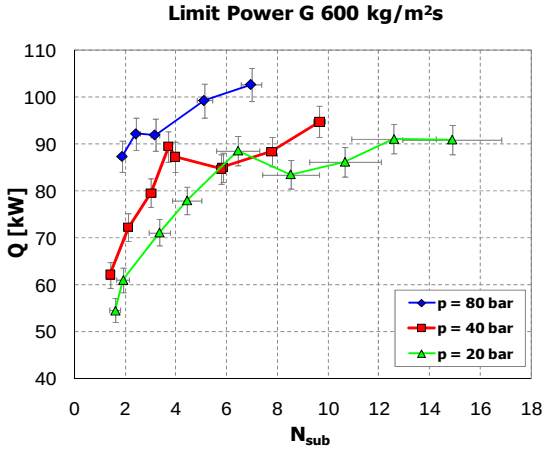

Figure 18 - Limit power for instability inception at G = 600 kg/m^{2}s as function of the subcooling number and at different pressures.

2.5.2 Period of oscillations and transit time

DWOs are characterized by waves of heavier and lighter fluid which travel alternatively along the boiling channel[3]. Two perturbations are required for each cycle. Accordingly, the period of oscillations should be of the order of twice the mixture transit time. As a matter of fact, literature results report a period of oscillation T almost equal to twice the mixture transit time τ at high inlet subcoolings, and a reduction of T/τ ratio by reducing the subcooling number [6]. In this respect, mixture transit time is considered calculated with classical homogeneous flow theory, by adding single-phase region transit time $\tau_{1\phi}$ and two-phase region transit time $\tau_{2\phi}$, as in [6] and [16]:

$$\tau = \tau_{1\varphi} + \tau_{2\varphi} = \frac{\overline{\rho_{in}}\Delta h_{in}}{q'''} + \frac{h_{lv}}{q'''v_{lv}}\ln\left(1+\frac{v_{lv}}{v_l}x_{ex}\right). \tag{3}$$

With some algebra, Eq. (3) can be rearranged as:

$$\tau = \frac{ALh_{lv}}{q}\left[-\overline{\rho_{in}}x_{in} + \frac{1}{v_{lv}}\ln\left(1+\frac{v_{lv}}{v_l}x_{ex}\right)\right]. \tag{4}$$

The experimental results collected at SIET labs show a completely different trend. The period of oscillations to transit time ratio is found to be very low at high inlet subcoolings, moreover it grows by reducing the subcooling number N_{sub}. The period of oscillations (Figure 19, Figure 21 and Figure 23) is rather independent on inlet subcooling, whereas it increases as the mass flow is lower. Accordingly, T/τ ratio (Figure 20, Figure 22 and Figure 24), pretty constant following mass flux variations, results considerably lower than one (~0.5) at high inlet subcoolings (when the fluid transit time in the heated channel is higher due to the long single-phase region), whereas it increases up to a value of nearly two as the inlet temperature approaches the saturation.

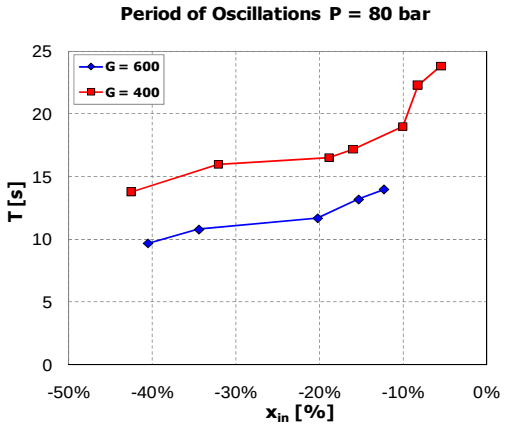

Figure 19 - Period of oscillations at p = 80 bar as function of inlet subcooling and for different values of mass flux.

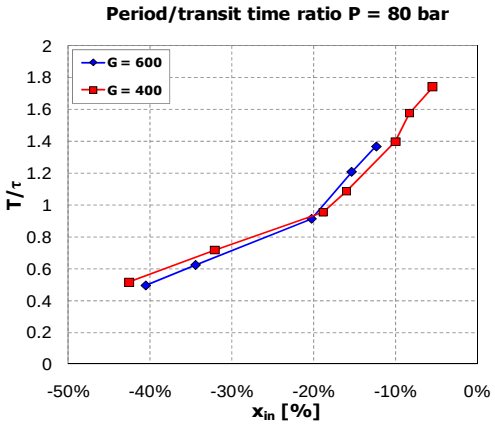

Figure 20 - Period of oscillations to transit time ratio at p = 80 bar as function of inlet subcooling and for different values of mass flux.

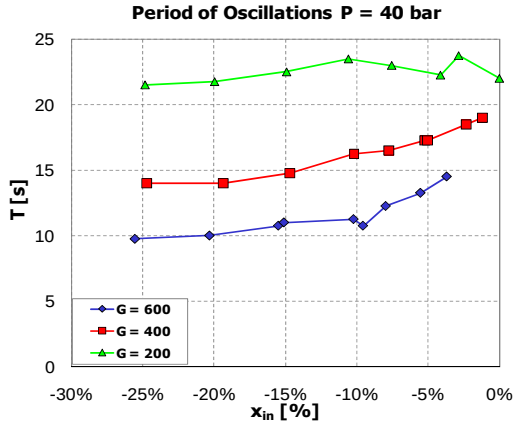

Figure 21 - Period of oscillations at p = 40 bar as function of inlet subcooling and for different values of mass flux.

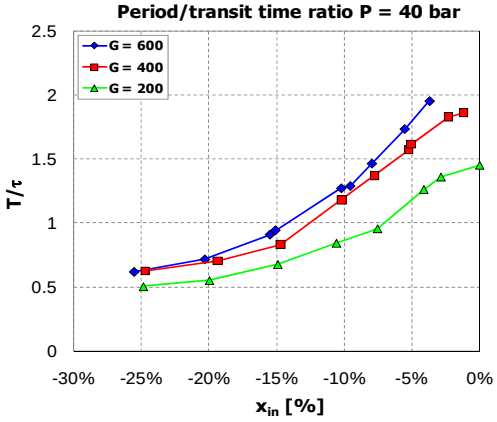

Figure 22 - Period of oscillations to transit time ratio at p = 40 bar as function of inlet subcooling and for different values of mass flux.

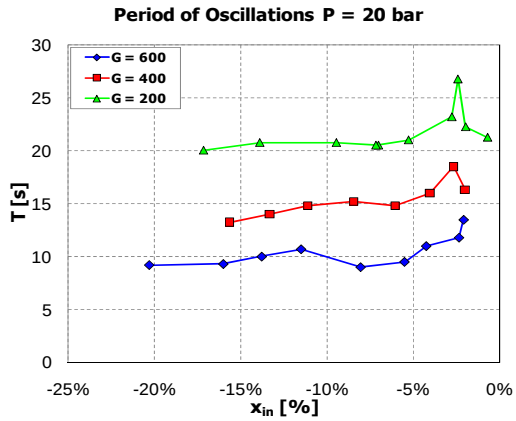

Figure 23 - Period of oscillations at p = 20 bar as function of inlet subcooling and for different values of mass flux.

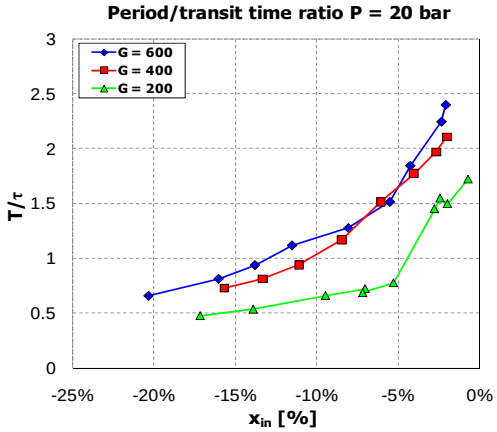

Figure 24 - Period of oscillations to transit time ratio at p = 20 bar as function of inlet subcooling and for different values of mass flux.

Up to the Authors knowledge, as well as from the helical geometry, the discussed behaviour seems to be induced also by the peculiar length of the test section and by the presence of an unheated riser above.

2.6 Effect of inlet throttling

It is well known that a concentrated pressure drop located at channel inlet is stabilizing, as a larger fraction of the system pressure drop behaves in-phase with inlet velocity variations [15]. In this work, the effect of inlet valve closure was investigated by repeating the stability map at p = 40 bar and G = 400 kg/m^{2}s, following progressive closures of V1 and V2 valves. All the results presented in the previous Sections have referred to "basically open" valve configuration (1 turn to valve closure, k_{in} = 45). In this paragraph, instead, the instability thresholds have been defined with respect to 2/6 turn to closure ($k_{in} \approx 100$) and 1/6 turn to closure ($k_{in} \approx 270$), respectively. Finally, a last position (roughly ascribable as 1/12 turn to valve closure) was tested, standing for the inlet throttling required to stabilize the parallel channel system under study. As a matter of fact, dryout thermal crisis occurrence was recorded before the onset of flow unstable

conditions, following the provided steps of thermal power. Hence, dryout occurrence, identified by a sharp rise of tube wall temperature, was considered as the evidence of system stabilization.

The obtained results are shown in Figure 25. The stabilizing effect of a concentrated pressure drop at the inlet of the channel is confirmed. Some explanations can be useful. When finding out the stability map at 1/6 turn to valve closure, asymmetric entrance resistance conditions were erroneously imposed by a not equal closure of the two valves (with Channel B less throttled than Channel A). It is shown that the stability characteristics of the less throttled (i.e., less stable) channel dominates the whole system. The instability occurs in the less throttled one, and then induces the other to oscillate. This reasoning is confirmed in literature by the experimental work of Guo Yun et al. [17]. To clarify this effect, some instability points were repeated with proper (i.e., balanced) closure between the two channel valves. A slight stabilization appears, as the system behaviour is effectively governed by the more throttled inlet valve configuration.

Nevertheless, the investigated effect of the inlet throttling on instability threshold turns out to be rather weak. By closing even remarkably the inlet valves, the system remained indeed prone to instability occurrence (with a global increase of the limit thermodynamic quality from ~0.5 to ~0.7, on the whole). Only a strong increase of the inlet throttling (with a concentrated pressure drop term that is such to equalize the distributed pressure drop term along the channel) permits to avoid the inception of the instability. Parallel channels stabilization given by the last position investigated (1/12 turn to valve closure) was not valid, indeed, at low subcooling; the respective threshold point is indicated on the stability map (Figure 25), with a limit quality equal to 0.8.

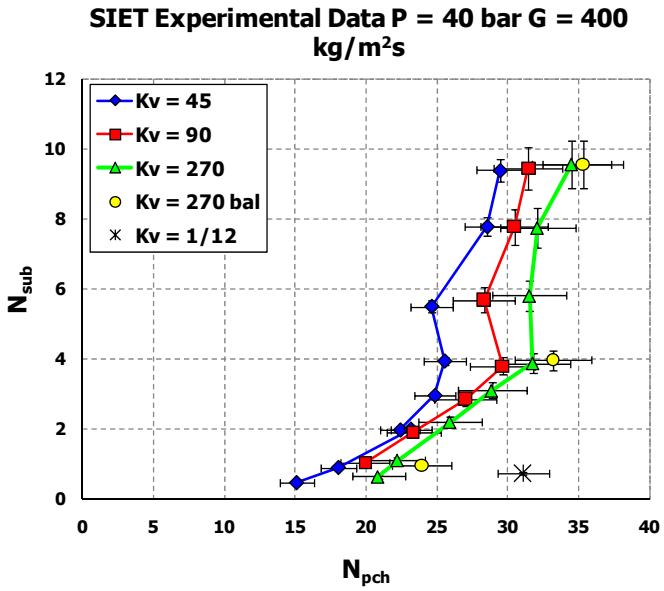

Figure 25 - Effect of inlet throttling on instability threshold at system pressure p = 40 bar and mass flux G = 400 kg/m^{2}s.

2.7 Ledinegg type instabilities

The final Section of the paper is dedicated to Ledinegg type instability. Ledinegg flow excursions were observed during test runs at the lowest pressure level (p = 20 bar), the highest mass flux (G = 600 kg/m^{2}s), and higher inlet subcooling values (x_{in} < -15%). Ledinegg type instabilities occur when a heated channel operates in the negative slope region of the pressure drop versus flow rate curve (channel characteristics). In this respect, the boundary conditions of constant

pressure drop given by parallel channels act as a flat pump external characteristics, forcing each channel into a wide flow excursion up to the reaching of new operating points on the internal characteristics.

Figure 26 shows the flow rate evolution in each channel in presence of a Ledinegg type instability. Flow excursion is evident, as Channel A flow rate increases. On the contrary, flow rate in Channel B reduces proportionally to preserve the imposed total mass flow rate. Constant total pressure drop condition is respected across the two tubes. Ledinegg instability occurrence showed to be critical since an anticipated DWO onset was recorded in the channel with lower flow rate (Channel B in this case), following small increases of supplied thermal power. Indeed, increase of thermal power permitted to leave the Ledinegg instability region, damping out the flow excursion.

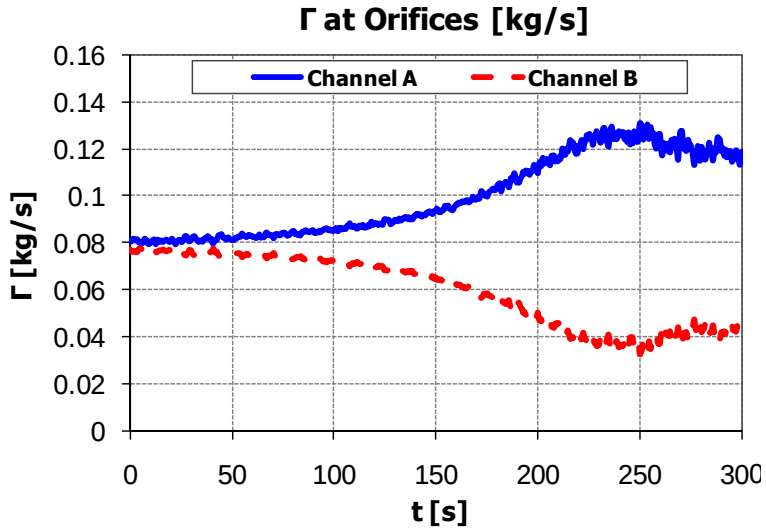

Figure 26 - Flow rate recorded in the two channels during a Ledinegg transient. Data collected with: p = 24 bar; T_{in} = 134 °C; G = 601 kg/m^{2}s. Transient to q = 50 kW (electrical power supplied per tube).

3 ANALYTICAL MODELLING

3.1 Analytical lumped parameter model: fundamentals and development

The analytical model provided to theoretically study DWO instabilities is based on the work of Muñoz-Cobo et al. [19]. Proper modifications have been considered to fit the modelling approach with steam generator tubes with imposed thermal power (representative of typical experimental facility conditions).

The developed model is based on a lumped parameter approach (0D) for the two zones characterizing a single boiling channel, which are single-phase region and two-phase region, divided by the boiling boundary. Modelling approach is schematically illustrated in Figure 27.

Differential conservation equations of mass and energy are considered for each region, whereas momentum equation is integrated along the whole channel. Wall dynamics is accounted for in the two distinct regions, following lumped wall temperature dynamics by means of the respective heat transfer balances. The model can apply to single boiling channel and two parallel channels configuration, suited both for instability investigation according to the specification of the respective boundary conditions:

- constant Δp across the tube for single channel;

- same $\Delta p(t)$ across the two channels (with constant total mass flow) for parallel channels [19].

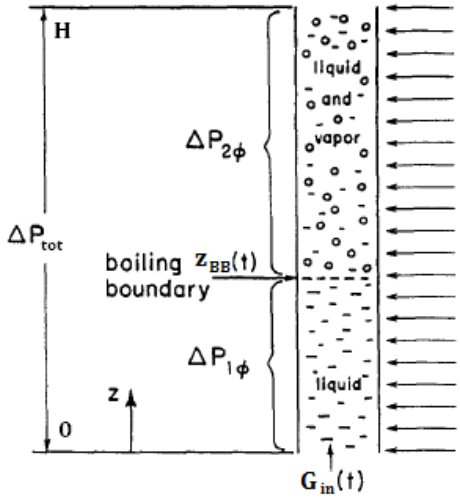

Figure 27 - Schematic diagram of a heated channel with single-phase ($0 < z < z_{BB}$) and two-phase ($z_{BB} < z < H$) regions. Externally impressed pressure drop is Δp_{tot}. (Adapted from [12]).

The main assumptions considered in the provided modelling are: (a) one-dimensional flow (straight tube geometry); (b) homogeneous two-phase flow model; (c) thermodynamic equilibrium between the two phases; (d) uniform heating along the channel (linear increase of quality with tube abscissa z); (e) system of constant pressure (pressure term is neglected within the energy equation); (f) constant fluid properties at given system inlet pressure; (g) subcooled boiling is neglected.

3.1.1 Mathematical modelling

Modelling equations are derived by the continuity of mass and energy for a single-phase fluid and a two-phase fluid, respectively.

Single-phase flow equations read:

$$\frac{\partial \rho}{\partial t} + \frac{\partial G}{\partial z} = 0\,, \tag{5}$$

$$\frac{\partial (\rho h)}{\partial t} + \frac{\partial (Gh)}{\partial z} = q'''\,. \tag{6}$$

Two-phase mixture is dealt with according to homogeneous flow model. By defining the homogeneous density ρ_H and the reaction frequency Ω as follows [18]:

$$\rho_H = \rho_l (1 - \bar{\alpha}) + \rho_v \bar{\alpha} = \frac{1}{v_l + \bar{x} v_{lv}}\,, \tag{7}$$

$$\Omega(t) = \frac{q(t)v_{lv}}{AHh_{lv}}, \tag{8}$$

one gets:

$$\frac{\partial \rho_H}{\partial t} + \frac{\partial G}{\partial z} = 0, \tag{9}$$

$$\frac{\partial j}{\partial z} = \Omega(t). \tag{10}$$

Momentum equation is accounted for by integrating the pressure balance along the channel:

$$\int_0^H \frac{\partial G(z,t)}{\partial t} dz = \Delta p(t) - \Delta p_{acc} - \Delta p_{grav} - \Delta p_{frict}. \tag{11}$$

As concerns the wall dynamics modelling, a lumped two-region approach is adopted. Heated wall dynamics is evaluated separately for single-phase and two-phase regions, following the dynamics of the respective wall temperatures according to a heat transfer balance:

$$\frac{dq^{1\varphi}}{dt} = M_h^{1\varphi} c_h \frac{dT_h^{1\varphi}}{dt} = q^{1\varphi} - (hS)^{1\varphi}\left(T_h^{1\varphi} - T_{fl}^{1\varphi}\right), \tag{12}$$

$$\frac{dq^{2\varphi}}{dt} = M_h^{2\varphi} c_h \frac{dT_h^{2\varphi}}{dt} = q^{2\varphi} - (hS)^{2\varphi}\left(T_h^{2\varphi} - T_{fl}^{2\varphi}\right). \tag{13}$$

3.1.2 Model development

Modelling equations are dealt with according to the usual principles of lumped parameter models [1], i.e. via integration of the governing PDEs (Partial Differential Equations) into ODEs (Ordinary Differential Equations) by applying the Leibniz rule. The hydraulic and thermal behaviour of a single heated channel is fully described by a set of 5 non-linear differential equations, in the form of:

$$\frac{dy_i}{dt} = f_i(y), \qquad i = 1, 2, ..., 5, \tag{14}$$

where the state variables are:

$$\begin{array}{lll} y_1 = z_{BB} & y_2 = x_{ex} & y_3 = G_{in} \\ y_4 = T_h^{1\phi} & y_5 = T_h^{2\phi} & \end{array}. \tag{15}$$

In case of single boiling channel modelling, boundary condition of constant pressure drop between channel inlet and outlet must be simply introduced by specifying the imposed Δp of interest within the momentum balance equation (derived following Eq. (12), see [1]).

In case of two parallel channels modelling, mass and energy conservation equations are solved for each of the two channels, while parallel channel boundary condition is dealt imposing within the momentum conservation equation: (a) the same pressure drop dependence with time ($\Delta p(t)$) across the two channels; (b) a constant total flow rate.

First, steady-state conditions of the analysed system are calculated by solving the whole set of equations with time derivative terms set to zero. Steady-state solutions are then used as initial conditions for the integrations of the equations, obtaining the time evolution of each computed state variable. Input variable perturbations (considered thermal power and channel inlet and exit loss coefficients according to the model purposes) can be introduced both in terms of step variations and ramp variations.

The described dynamic model has been solved through the use of the MATLAB software SIMULINK® [32].

3.1.3 Linear stability analysis

Modelling equations can be linearized to investigate the neutral stability boundary of the nodal model. The linearization about an unperturbed steady-state initial condition is carried out by assuming for each state variable:

$$y(t) = y^0 + \delta y \cdot e^{\lambda t} . \tag{16}$$

To simplify the calculations, modelling equations are linearized with respect to the three state variables representing the hydraulic behaviour of a boiling channel, i.e. the boiling boundary $z_{BB}(t)$, the exit quality $x_{ex}(t)$, and the inlet mass flux $G_{in}(t)$. That is, linear stability analysis is presented by neglecting the dynamics of the heated wall ($q(t)$ = const).

The initial ODEs, obtained after integration of the original governing PDEs, are [1]:

$$\frac{dz_{BB}}{dt} = b_1 , \tag{17}$$

$$\frac{dx_{ex}}{dt} = b_4 = b_2 + b_3 \frac{dz_{BB}}{dt} , \tag{18}$$

$$\frac{dG_{in}}{dt} = b_5 . \tag{19}$$

By applying Eq. (16) to the selected three state variables, as:

$$z_{BB}(t) = z_{BB}^0 + \delta z_{BB} \cdot e^{\lambda t} , \tag{20}$$

$$x_{ex}(t) = x_{ex}^0 + \delta x_{ex} \cdot e^{\lambda t} , \tag{21}$$

$$G_{in}(t) = G_{in}^0 + \delta G_{in} \cdot e^{\lambda t} , \tag{22}$$

the resulting linear system can be written in the form of:

$$\delta z_{BB} E_{11} + \delta x_{ex} E_{12} + \delta G_{in} E_{13} = 0 \,, \tag{23}$$

$$\delta z_{BB} E_{21} + \delta x_{ex} E_{22} + \delta G_{in} E_{23} = 0 \,, \tag{24}$$

$$\delta z_{BB} E_{31} + \delta x_{ex} E_{32} + \delta G_{in} E_{33} = 0 \,. \tag{25}$$

The calculation of the system eigenvalues is based on solving:

$$\begin{vmatrix} E_{11} & E_{12} & E_{13} \\ E_{21} & E_{22} & E_{23} \\ E_{31} & E_{32} & E_{33} \end{vmatrix} = 0 \,, \tag{26}$$

which yields a cubic characteristic equation, where λ are the eigenvalues of the system:

$$\lambda^3 + a\lambda^2 + b\lambda + c = 0 \,. \tag{27}$$

3.2 Analytical lumped parameter model: results and discussion

Single boiling channel configuration is referenced for the discussion of the results obtained by the developed model on DWOs. For the sake of simplicity, and availability of similar works in the open literature for validation purposes [19][21][25], typical dimensions and operating conditions of classical BWR core subchannels are considered.
Table 4 lists the geometrical and operational values taken into account in the following analyses.

Table 4 - Dimensions and operating conditions selected for the analyses.

Heated Channel	
Diameter [m]	0.0124
Length [m]	3.658
Operating Parameters	
Pressure [bar]	70
Inlet temperature [°C]	151.3 – 282.3
k_{in}	23
k_{out}	5

3.2.1 System transient response

To excite the unstable modes of density wave oscillations, input thermal power is increased starting from stable stationary conditions, step-by-step, up to the instability occurrence. Instability threshold crossing is characterized by passing through damping out oscillations (Figure 28), limit cycle oscillations (Figure 29), and divergent oscillations (Figure 30). This process is rather universal across the boundary. From stable state to divergent oscillation state, a narrow transition zone of some kW has been found in this study.

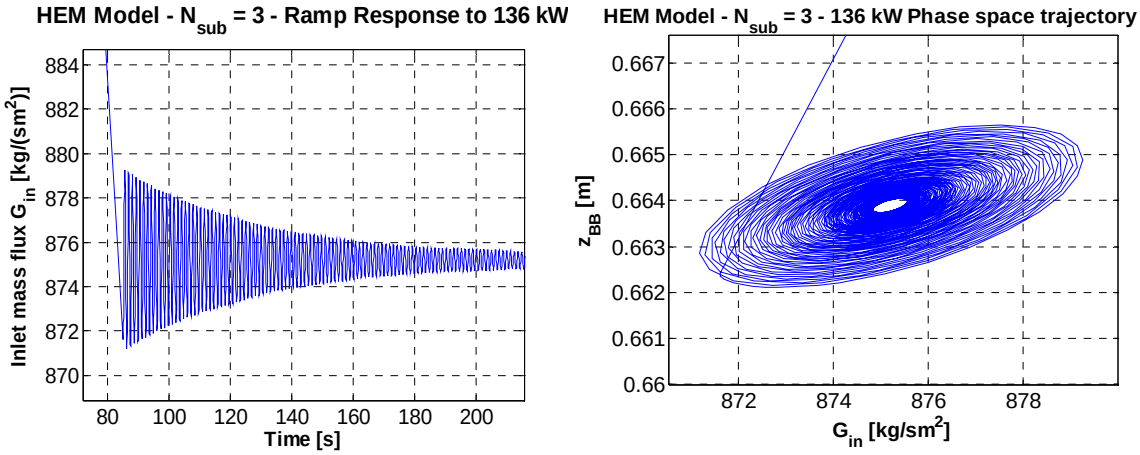

Figure 28 - Inlet mass flux oscillation curves and corresponding trajectories in the phase space for a stable state.

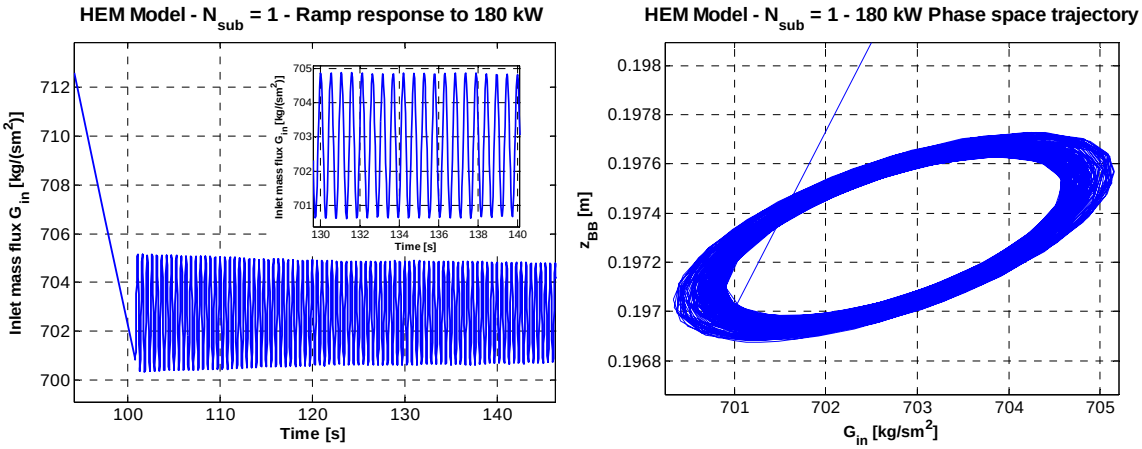

Figure 29 - Inlet mass flux oscillation curves and corresponding trajectories in the phase space for a point on the neutral stability boundary.

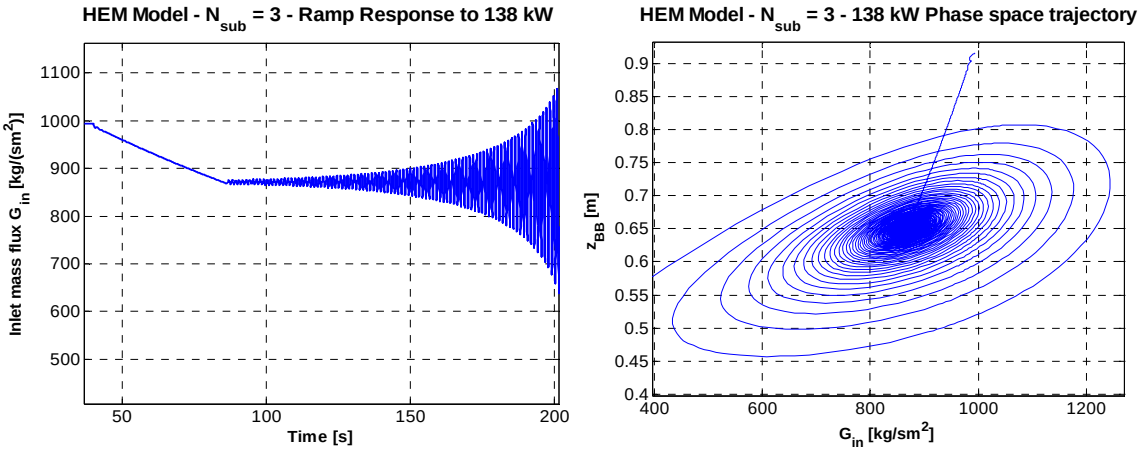

Figure 30 – Inlet mass flux oscillation curves and corresponding trajectories in the phase space for an unstable state.

The analysed system is non-linear and pretty complex. Trajectories on the phase space defined by boiling boundary z_{BB} vs. inlet mass flux G_{in} are reported in Figure 28, Figure 29 and Figure 30 too. The operating point on the stability

boundary (Figure 29) is the cut-off point between stable (Figure 28) and unstable (Figure 30) states. This point can be looked as a bifurcation point. The limit oscillation is a quasi-periodic motion; the period of the depicted oscillation is rather small (less than 1 s), due to the low subcooling conditions considered at inlet.

With reference to the eigenvalue computation, by solving Eq. (27), at least one of the eigenvalues is real, and the other two can be either real or complex conjugate. For the complex conjugate eigenvalues, the operating conditions that generate the stability boundary are those in which the complex conjugate eigenvalues are purely imaginary (i.e., the real part is zero). Crossing the instability threshold is characterized by passing to positive real part of the complex conjugate eigenvalues, which is at the basis of the diverging response of the model under unstable conditions.

3.2.2 Description of a self-sustained DWO

The simple two-node lumped parameter model developed in this work is capable to catch the basic phenomena of density wave oscillations. Numerical simulations have been used to gain insight into the physical mechanisms behind DWOs, as discussed in this paragraph.

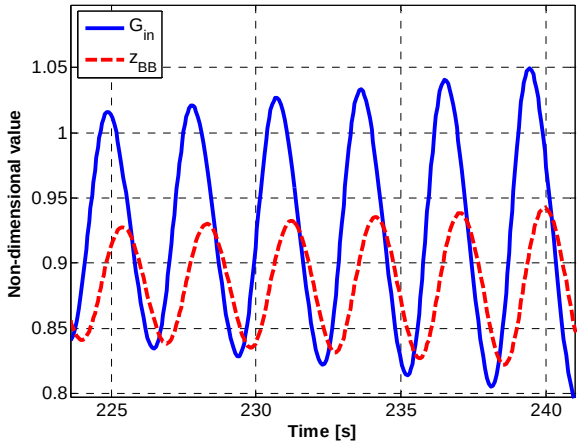

Figure 31 - Dimensionless inlet mass flux and boiling boundary. N_{sub} = 8, q = 133 kW.

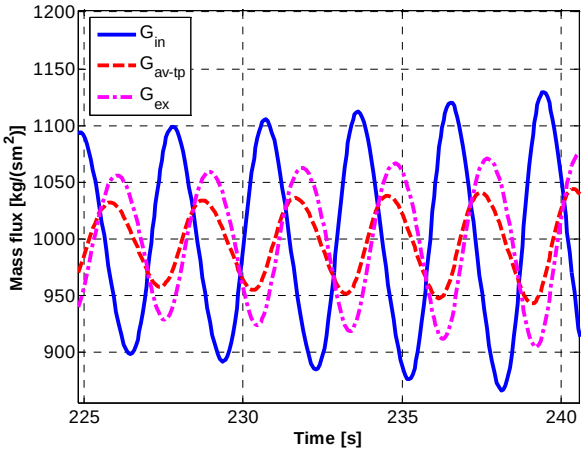

Figure 32 - Mass flux delayed variations along the channel. N_{sub} = 8, q = 133 kW.

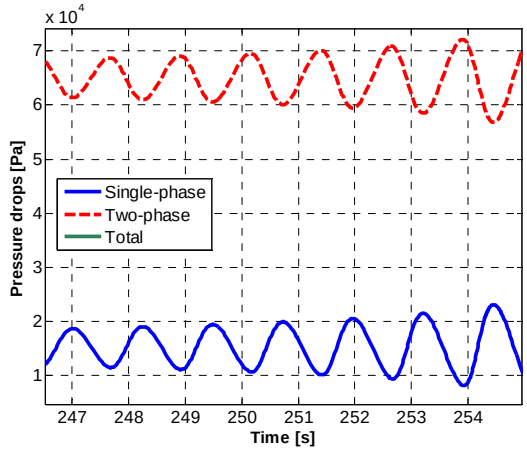

Figure 33 - Oscillating pressure drop distribution. N_{sub} = 2, q = 103 kW.

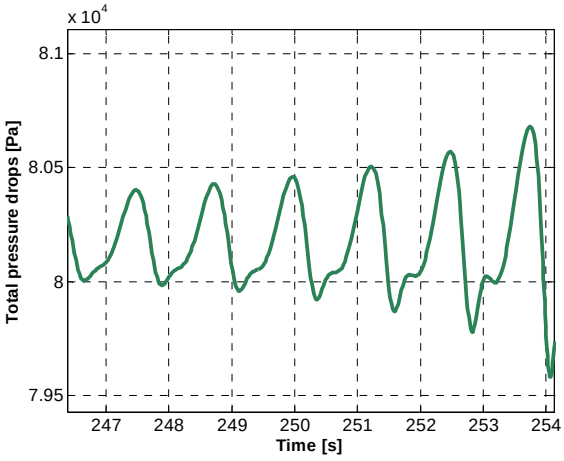

Figure 34 - "Shark-fin" oscillation of total pressure drops. N_{sub} = 2, q = 103 kW.

The analysis has shown good agreement with some findings due to Rizwan-uddin [12]. Fully developed DWO conditions are considered. By analyzing an inlet velocity variation and its propagation throughout the channel, particular features of the transient pressure drop distributions are depicted.

The starting point is taken as a variation (increase) in the inlet velocity. The boiling boundary responds to this perturbation with a certain delay (Figure 31), due to the propagation of an enthalpy wave in the single-phase region. The propagation of this perturbation in the two-phase zone (via quality and void fraction perturbations) causes further lags in terms of two-phase average velocity and exit velocity (Figure 32).

All these delayed effects combine in single-phase pressure drop term and two-phase pressure drop term acquiring 180° out-of-phase fluctuations (Figure 33). What is interesting to notice, indeed, is that the 180° phase shift between single-phase and two-phase pressure drops is not perfect [12]. Due to the delayed propagation of initial inlet velocity variation, single-phase term increase is faster than two-phase term rising. The superimposition of the two oscillations (in some operating conditions) is such to create a total pressure drop along the channel oscillating as a non-sinusoidal wave. The peculiar trend obtained is shown in Figure 34; relating oscillation shape has been named "shark-fin" shape. Such behaviour has found corroboration in the experimental evidence collected with the facility at SIET labs [2]. In Figure 35 an experimental recording of channel total pressure drops is depicted. The experimental pressure drop oscillation shows a fair qualitative agreement with the phenomenon of "shark-fin" shape described theoretically.

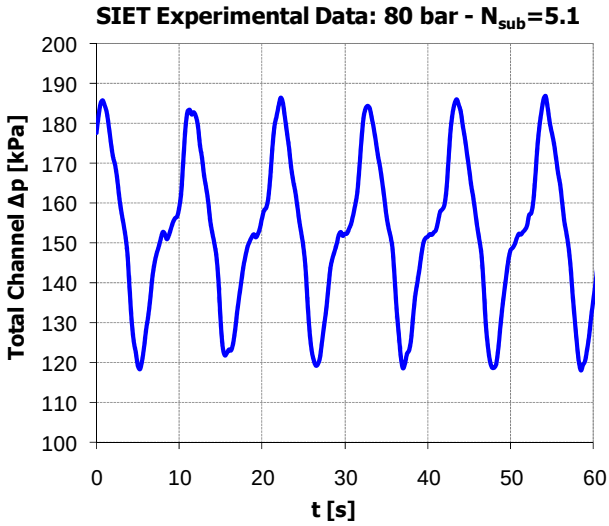

Figure 35 - Experimental recording of total pressure drop oscillation showing "shark-fin" shape (SIET labs).

3.2.3 Sensitivity analyses and stability maps

In order to provide accurate quantitative predictions of the instability thresholds, and of their dependence with the inlet subcooling to draw a stability map (as the one commonly drawn in the N_{pch}–N_{sub} stability plane [13], see e.g. Figure 2), it is first necessary to identify most critical modelling parameters that have deeper effects on the results.

Several sensitivity studies have been carried out on the empirical coefficients used to model two-phase flow structure. In particular, specific empirical correlations have been accounted for within momentum balance equation to represent two-phase frictional pressure drops (by testing several correlations for the two-phase friction factor multiplier Φ_{lo}^2).

In this respect, a comparison of the considered friction models is provided in Table 5: Homogeneous Equilibrium pressure drop Model (HEM), Lockhart-Martinelli multiplier, Jones expression of Martinelli-Nelson method and Friedel correlation are selected [33], respectively, for the analysis. It is worth noticing that the main contribution to channel total pressure drops is given by the two-phase terms, both frictional and in particular concentrated losses at channel exit (nearly 40-50%). Fractional distribution of the pressure drops along the channel plays an important role in determining the stability of the system. Concentration of pressure drops near the channel exit is such to render the system prone to instability: hence, DWOs triggered at low qualities may be expected with the analysed system.

Table 5 - Fractional contributions to total channel pressure drop (at steady-state conditions).

Test case: $\Gamma = 0.12$ kg/s; $T_{in} = 239.2$ °C; $q = 100$ kW ($x_{ex} = 0.40$)

	HEM		**Lockhart-Martinelli**		**Jones**		**Friedel**	
Term	*Δp [kPa]*	*% of total*	*Δp [kPa]*	*% of total*	*Δp [kPa]*	*% of total*	*Δp [kPa]*	*% of total*
Δp_{grav}	12.82	17.31%	12.82	7.96%	12.82	10.96%	12.82	14.62%
Δp_{acc}	10.24	13.84%	10.24	6.36%	10.24	8.76%	10.24	11.68%
Δp_{in}	15.35	20.74%	15.35	9.54%	15.35	13.12%	15.35	17.51%
$\Delta p_{frict,1\varphi}$	0.96	1.29%	0.96	0.59%	0.96	0.82%	0.96	1.09%
$\Delta p_{frict,2\varphi}$	10.61	14.33%	39.84	24.75%	23.54	20.12%	14.97	17.07%
Δp_{ex}	24.06	32.50%	81.73	50.79%	54.07	46.22%	33.36	38.04%
Δp_{tot}	74.03	100%	160.94	100%	116.97	100%	87.69	100%

The effects of two-phase frictions on the instability threshold are evident from the stability maps shown in Figure 36. The higher are the two-phase friction characteristics of the system (that is, with Lockhart-Martinelli and Jones models), the most unstable results the channel (being the instability induced at lower thermodynamic quality values). Moreover, RELAP5 calculations about DWO occurrence in the same system are reported as well [5]. In these conditions, Friedel correlation for two-phase multiplier is the preferred one.

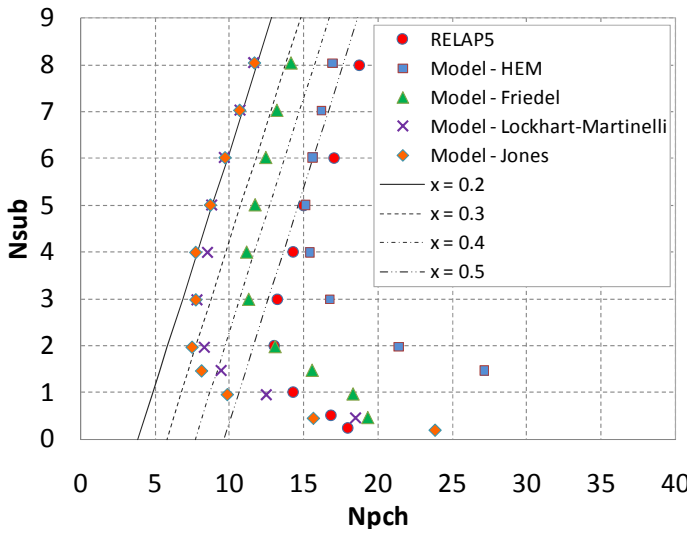

Figure 36 - Stability maps in the N_{pch}–N_{sub} stability plane, drawn with different models for two-phase friction factor multiplier.

The influence of the two-phase friction multiplier on the system stability (via the channel pressure drop distribution) is made apparent also in terms of eigenvalues computation. Figure 37 reports the results of the linear stability analysis corresponding to the four cases depicted in Table 5.

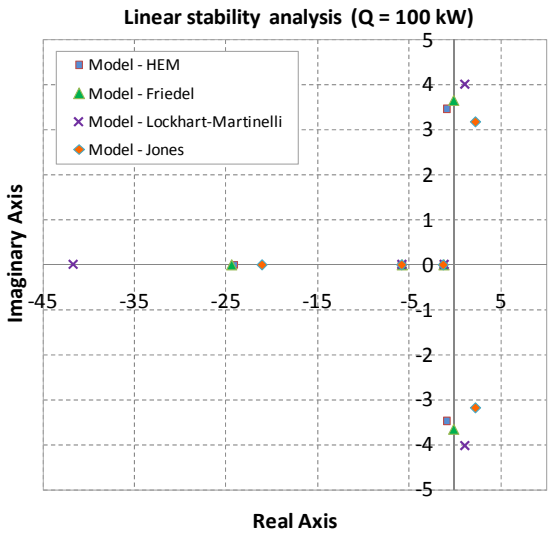

Figure 37 - Sensitivity on two-phase friction factor multiplier in terms of system eigenvalues. Test case: $\Gamma = 0.12$ kg/s; $T_{in} = 239.2$ °C; $q = 100$ kW ($x_{ex} = 0.40$).

4 NUMERICAL MODELLING BY MEANS OF RELAP5 CODE

Capability of the RELAP5/MOD3.3 [24] system code to detect the appearance of density wave oscillations in a single boiling channel has been studied in [5]. A single channel configuration was addressed by working with an imposed Δp, kept constant throughout the simulation. Moreover a more realistic experimental apparatus for DWO investigation was reproduced, connecting a bypass tube to the heated channel to maintain the constant pressure drop boundary condition. The RELAP5 code demonstrated its capability to correctly detect the onset of instability. A sufficiently large bypass permitted to reproduce the same results obtained with single channel alone simulations. In this section the analysis is extended studying twin parallel channels.

4.1 Model and numerical settings

A description of the two parallel channels nodalization developed in RELAP5 is provided in Figure 38. With respect to [5], a twin channel is added to the system, with connection through common lower and upper headers. Uniform equal heating along the two channel axes is considered. Initially physical parameters and tube size are kept equal to the values of a typical BWR subchannel (Table 6). Then, the two channels are modified to fit with facility helical coil tubes. The real dimensions of the experimental facility are indicated in Table 1.

Because only straight pipe elements are implemented in the code and all the models and correlations refer to straight geometry, a fictitious configuration is introduced. Two straight inclined tubes are assumed, with the same inclination of the helical coil, in order to reproduce both tube length and height of the facility. Moreover, no local pressure losses at the exit of the channels have been considered.

Table 6 - RELAP5 parameters for BWR geometry simulation.

Heated Channel	
Diameter [m]	0.0124
Length [m]	3.658
Roughness [m]	$2.5 \cdot 10^{-5}$
Operating parameters	
Exit pressure [Pa]	$7.0 \cdot 10^{6}$
Inlet temperatures [°C]	151.3 - 282.3
k_{in}	23
k_{ex}	5

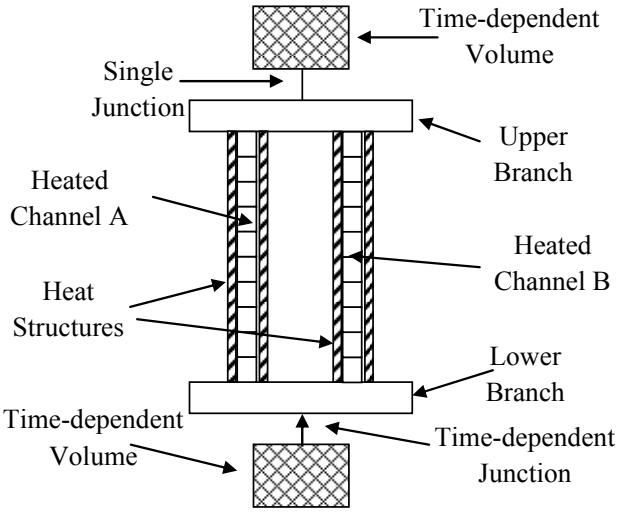

Figure 38 - RELAP5 nodalization of two parallel tubes with common lower and upper headers.

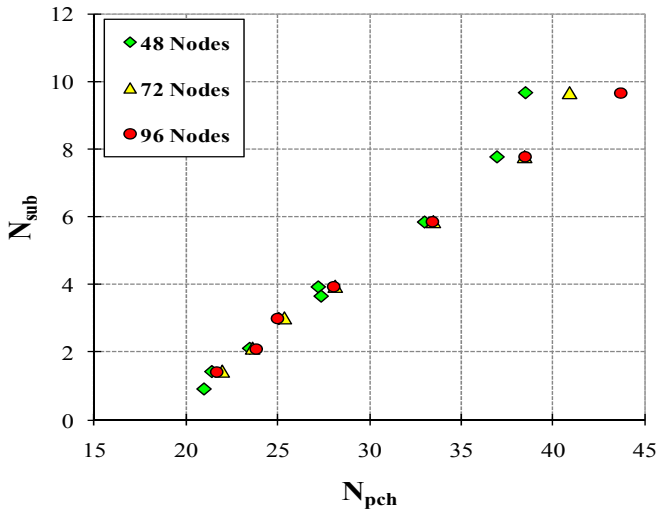

Figure 39 - Stability maps obtained in two parallels channels with different nodalizations (p = 40 bar, G = 600 kg/m^{2}s, 155°C < T_{in}< 238°C, L = 32 m).

Code models and numerical settings are exactly the same as in [5], thus UVUT model, semi-implicit numerical scheme and a time step always equal to the 95% of the Courant limit. Conversely, after a sensitivity study shown in Figure 39, the number of nodes has been increased to 96 for the 32 m long duct.

The following procedure is adopted to reach the instability boundary: at the beginning of each run specific values of exit pressure, mass flow rate and inlet water temperature are selected as initial conditions. Flow circulation in the system starts at zero power, then power generation in the heat structures is increased gradually till the unstable condition is reached. The increase rate is higher at the beginning of the transient, to quickly approach the unstable region, then it is lowered to guarantee an easier detection of the onset of instability.

4.2 Results and discussion

4.2.1 BWR subchannel geometry

In a system of two parallel channels, density wave instability occurs with counter-phase oscillations of the flow rate in the two channels (Figure 40). Total system mass flow rate remains constant, being imposed by a pump.

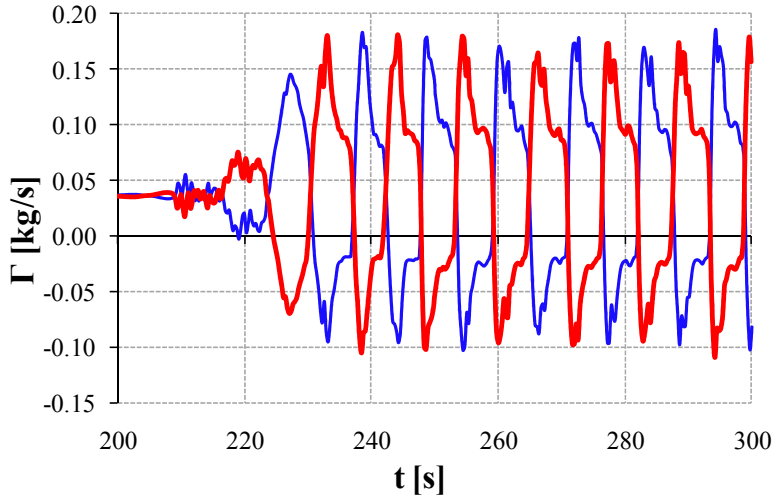

Figure 40 - Mass flow rate oscillating in counter-phase during a fully-developed DWO in parallel channels.

Stability map for two parallel tubes is shown in Figure 41, where it is compared to the stability thresholds of the single channel [5]. Except for small deviations at low inlet subcooling, density wave instability exhibits the same behaviour in the three different systems. Hereby, with the correct settings, RELAP5 shows satisfactory prediction capability with respect to DWOs also in a parallel channel system featuring the simple geometry of BWR subchannel.

Some remarks are needed on the determination of the exact point where the system crosses the stability boundary and, consequently, has to be considered unstable. A typical transient is shown in Figure 42. Mass flow rate decreases with time as the supplied power is increased, until it starts to oscillate when the instability threshold is approached. Clearly, no universal detection criteria exist. In this work the system was considered unstable when mass flow rate oscillation amplitude reached 100% of the steady-state value. For verification purposes, the same results were analyzed according to a visual detection criterion, in which the system was considered unstable when mass flow rate oscillation appeared

fully-developed. The visual detection was viable thanks to the almost flat power ramps imposed near instability inception (causing the mass flow rate to vary slightly).

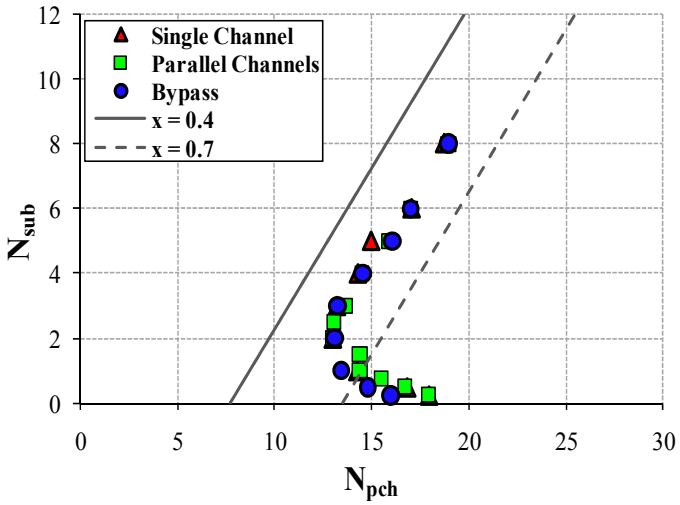

Figure 41 - Comparison between the stability maps calculated with the three different system configurations studied in BWR subchannel geometry.

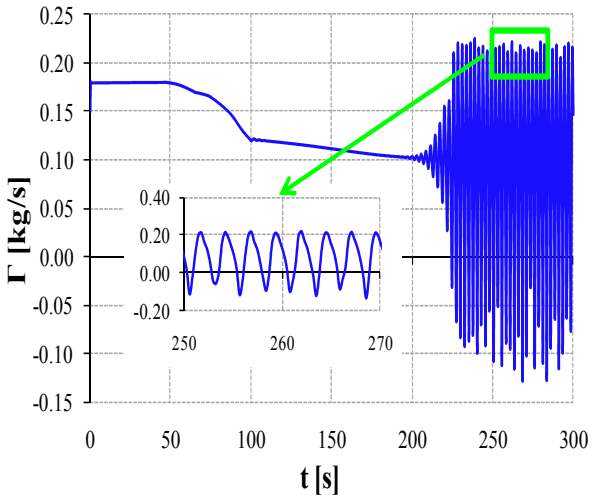

Figure 42 - Mass flow rate behavior in the heated channel during a DWO.

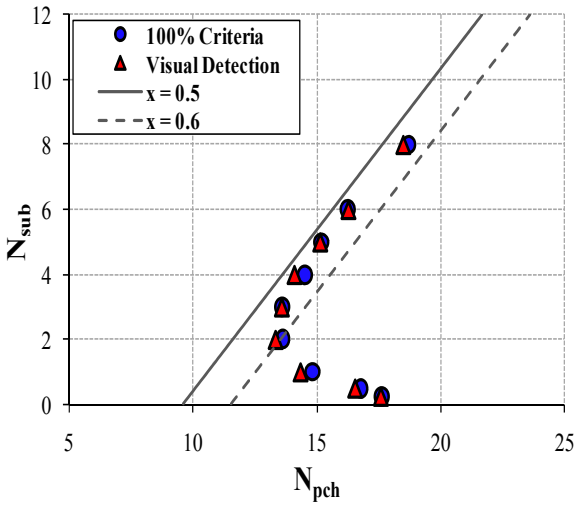

Figure 43 - Comparison between a visual detection criterion and a more precise one, based on 100% of steady-state value oscillation amplitude to consider unstable the system.

As it is shown in Figure 43, no significant differences were found. Hereby, all the results are presented in the followings by using the 100% detection criterion.

4.2.2 Parametric study

For future comparisons between RELAP5 predictions and the experimental data with helical coil geometry, a RELAP5 model reproducing as far as possible the experimental facility has been developed. In this Section, tube length and inclination were modified from the BWR subchannel geometry one by one, to study their influence on the system stability. System operating parameters have been assumed as in Table 6.

The system exhibits a marked stabilization when increasing the length of the channel maintaining the inclination fixed (straight vertical duct). In Figure 44 three different tube lengths are presented: BWR subchannel (3.66 m), experimental facility tube (32 m), and vertical channel with length equal to the height of the experimental facility (8 m). Obviously, the stabilization is larger passing from 8 m to 32 m. The effect of tube length appears somewhat strange, because it is expected to increase of the same relative amount both frictional and gravitational pressure terms, which are proportionally to tube length. Although gravitational pressure drops are not negligible in a straight vertical tube, one expects two-phase frictional pressure losses to be the most important term in total pressure drop balance. An increase in two-phase frictional pressure losses, concentrating the pressure drop near the channel exit, is expected to increase system propensity to instability [12][34].

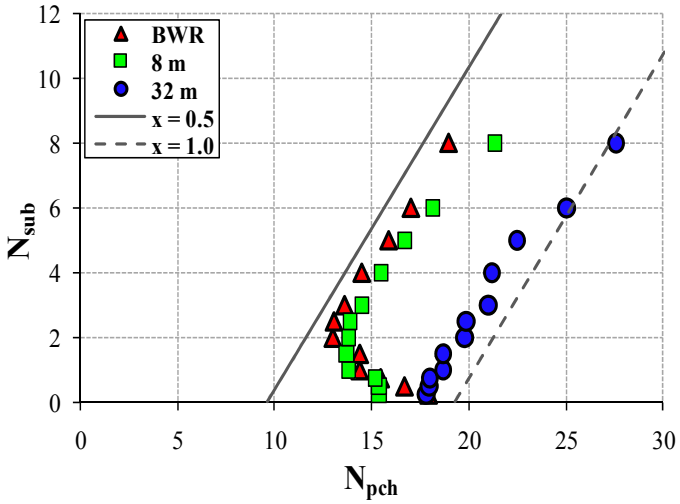

Figure 44 - Stability maps obtained in parallel channels with different values of channel length.

When only a single channel is considered, tube length influence seems to disappear (Figure 45) and the stability threshold remains almost unchanged. The latter result could suggest some difficulties of the RELAP5 code in addressing more complex geometry (as the stabilization highlighted in Figure 44 when increasing tube length could be induced just by numerical diffusion introduced to assure convergence of the calculations). Figure 46 reports the stability maps obtained with RELAP5 varying tube inclination while maintaining fixed the channel length. The stable region widens as the tube approaches the vertical orientation (starting from horizontal duct). An increase in inclination (hence from horizontal to vertical duct) turns out in a higher gravitational pressure drop term, concentrated in the single-phase region, where higher is the density of the fluid. Increase in single-phase region pressure drop, close to channel inlet section, reinforces system stability. As concerns tube inclination, the RELAP5 code shows the capability to qualitatively reproduce its physical influence on instability inception.

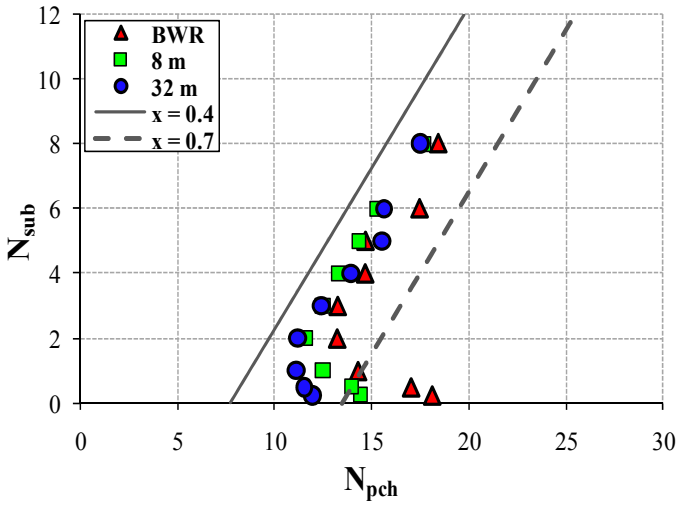

Figure 45 - Stability maps obtained in single channel with different values of channel length.

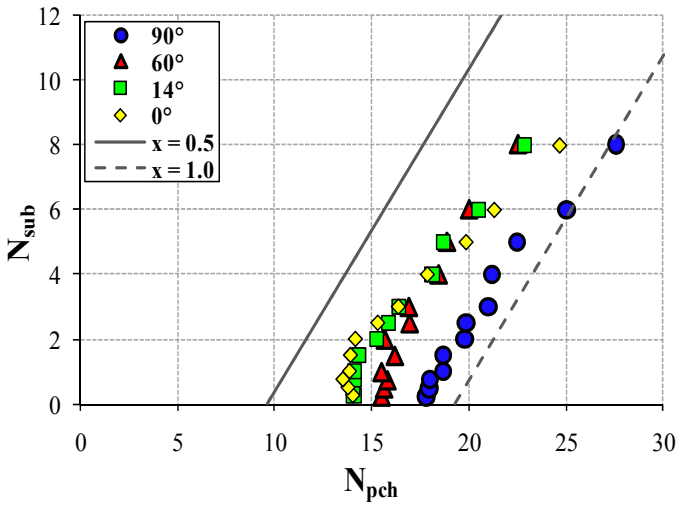

Figure 46 - Stability maps obtained in parallel channels with different values of channel inclination.

5 NUMERICAL MODELLING BY MEANS OF COMSOL CODE

5.1 Mathematical formulation and model development

COMSOL Multiphysics® [26] is a numerical code which is gaining importance in the recent years, based on its possibility to solve different numerical problems by implementing directly the systems of equations in PDE form. PDEs are then solved numerically by means of finite element techniques. It is mentioned that this approach is globally different from previous one discussed (i.e., the RELAP5 code), which indeed considers finite volume discretizations of the governing equations, and of course from the simple analytical treatment thoroughly discussed in Section 3.

Modelling equations, derived from conservation of mass, energy and momentum, have been implemented separately with respect to single-phase region and two-phase region.

In single-phase region, the mass, momentum and energy balance equations take, for a typical physical system, the following form:

$$\frac{\partial \rho}{\partial t} + \frac{\partial G}{\partial z} = 0 \,, \tag{28}$$

$$\frac{\partial G}{\partial t} + \frac{\partial}{\partial z}\left(\frac{G^2}{\rho}\right) = -\frac{\partial p}{\partial z} - \rho g \sin\theta - \left(\frac{\partial p}{\partial z}\right)_{frict} \,, \tag{29}$$

$$\frac{\partial}{\partial t}\left(\rho h - p + \frac{G^2}{2\rho}\right) + \frac{\partial}{\partial z}\left(Gh + \frac{G^3}{2\rho^2}\right) = \frac{q'' H}{A} + \frac{G}{\rho}\left(\frac{\partial p}{\partial z}\right)_{frict} - Gg \sin\theta \,. \tag{30}$$

The physical system represented in Eqs.(28) – (30) is made by a straight tube of length *H*, circular cross-section of diameter *D* and slope angle θ (between tube axis and the horizontal direction). Of course, $\sin\theta = 1$ applies in order to simulate the straight vertical BWR subchannel under investigation (Table 4).

A simpler enthalpy balance equation can replace Eq.(30), by subtracting a convenient form of Eq.(29) from Eq.(30). One obtains:

$$\frac{\partial}{\partial t}(\rho h - p) + \frac{\partial}{\partial z}(Gh) = \frac{q'' H}{A} + \frac{G}{\rho}\left[\left(\frac{\partial p}{\partial z}\right)_{frict} + \frac{\partial p}{\partial z}\right] \,. \tag{31}$$

In two-phase region, the mass, momentum and energy balance equations read:

$$\frac{\partial \rho_m}{\partial t} + \frac{\partial G}{\partial z} = 0 \,, \tag{32}$$

$$\frac{\partial G}{\partial t} + \frac{\partial}{\partial z}\left(\frac{G^2}{\rho_m^+}\right) = -\frac{\partial p}{\partial z} - \rho_m g \sin\theta - \left(\frac{\partial p}{\partial z}\right)_{frict}^{2\varphi} \,, \tag{33}$$

$$\frac{\partial}{\partial t}\left(\rho_m h_m - p + \frac{G^2}{2\rho_m^+}\right) + \frac{\partial}{\partial z}\left(Gh_m^+ + \frac{G^3}{2\rho_m^{+2}}\right) = \frac{q'' H}{A} + \frac{G}{\rho_m}\left(\frac{\partial p}{\partial z}\right)_{frict}^{2\varphi} - Gg \sin\theta \,. \tag{34}$$

Alike the single-phase region equations, an enthalpy balance equation is more convenient than Eq.(34). Hence, the kinetic energy terms within Eq.(34) can be eliminated by subtracting Eq.(33). One finally obtains:

$$\frac{\partial}{\partial t}(\rho_m h_m - p) + \frac{\partial}{\partial z}\left(Gh_m^+\right) = \frac{q'' H}{A} + \frac{G}{\rho_m}\left[\left(\frac{\partial p}{\partial z}\right)_{frict}^{2\varphi} + \frac{\partial p}{\partial z}\right] \,. \tag{35}$$

Though fundamentally similar to single-phase region equations, two-phase flow conservation equations require proper definition of the two-phase flow structure. In particular, suited expressions for static and dynamic two-phase density and enthalpy, as well as for two-phase frictional term (via the two-phase friction multiplier Φ_{lo}^2 concept), must be considered. General expressions for the terms representing a two-phase mixture are given by:

$$\rho_m = \alpha\rho_v + (1-\alpha)\rho_l , \tag{36}$$

$$\rho_m^+ = \left[\frac{x^2}{\alpha\rho_v} + \frac{(1-x)^2}{(1-\alpha)\rho_l}\right]^{-1} , \tag{37}$$

$$h_m = \frac{\alpha\rho_v h_v + (1-\alpha)\rho_l h_l}{\rho_m} , \tag{38}$$

$$h_m^+ = xh_v + (1-x)h_l . \tag{39}$$

The widespread $S-\alpha-x$ relation is used to relate the previous quantities:

$$\alpha = \left[1 + \frac{1-x}{x}\frac{\rho_v}{\rho_l}S\right]^{-1} . \tag{40}$$

The value of the slip ratio S depends on the choice of the two-phase flow model adopted. In this Section, both a simple homogeneous flow model (S = 1, as the assumption on which basis the analytical lumped parameter model has been derived, see Par. 3.1.1), and a more accurate Drift-Flux Model (DFM) have been considered. The latter accounts for the effect of the relative velocity between the two phases (the so-named slip), by defining a suitable slip ratio S as follows:

$$S = C_0 + \frac{(C_0-1)x\rho_l}{(1-x)\rho_v} + \frac{V_{vj}\rho_l}{(1-x)G} . \tag{41}$$

The quantities C_0 and V_{vj} indicate respectively the concentration parameter (void distribution parameter) and the effective drift-flux velocity. The first represents the global effect due to non-uniform void distribution and velocity profiles in the channel section, whereas the latter represents the local relative velocity effect and generally depends on the flow regime.

Several correlations exist for the two parameters. Various combinations of drift-flux models, together with different two-phase friction multiplier expressions, have been tested. Comprehensive results can be found in the master thesis of Giorgi [35]. For the aims of this paper, just the simple DFM based on a constant value of the concentration parameter (C_0 = 1.13) [9] and Lahey and Moody correlation for the drift-flux velocity [33] are considered. HEM model is implemented with homogeneous Φ_{lo}^2, whereas DFM is implement with Jones correlation for Φ_{lo}^2 (both already utilized in the analytical model in Section 3.2.3).

Implementation of the modelling equations set has been carried out using the PDE General Form module of COMSOL Multiphysics®. The obtained 1D thermal hydraulic simulator works out switching between single-phase and two-phase region according to a selection logic that considers the following check variable v_c:

$$v_c = \frac{h_m^+ - h_l}{h_v - h_l} . \tag{42}$$

The value of v_c (basically representing the thermodynamic quality x) is evaluated in each node. Single-phase zone equations are accounted for if $v_c < 0$ or $v_c > 1$, whereas two-phase zone equations are accounted for if $0 \le v_c \le 1$. Similar computational procedure is followed, for instance, in the work of Colorado et al. [36].

5.2 Results and discussion

Steady-state predictions from the described modelling with COMSOL code have been firstly validated, before any attempt to apply this numerical modelling tool for the study of density wave instabilities.

Experimental test-case for the 1D simulator built-up with the COMSOL code has been represented by the thorough pressure drop database obtained by Santini [37] and Santini et al.[28], who worked on the helical coiled tube test section, located at SIET labs and pioneering to the experimental activities on DWO threshold characterization carried out by Papini et al. [2].

COMSOL thermal-hydraulic simulator has been adapted to the peculiar referenced geometry, on the account of specific modifications including e.g. the approximation with a straight inclined channel, long as the helical tube and with the same inclinational angle θ of the facility helix [3].

The comparison between the numerical predictions and the experimental pressure drop data on the helical coil facility is depicted in Figure 47 (respectively for three different pressure levels). The agreement is satisfactory, with maximum error less than 10%.

As final step, the water-steam thermal hydraulic simulator has been applied to boiling channel stability analysis, via linearization of the equation system (Eqs.(28) – (35)) and computation of the eigenvalues, on the basis of the experience collected in Section 2.3. Just the single boiling channel case is hereby presented. COMSOL Eigenvalue Solver has been used, yielding the linearization of the equations about an equilibrium point. The linearization tool acts by substituting each temporal derivative operator in the following way:

$$\frac{\partial}{\partial t} \longrightarrow -\lambda, \tag{43}$$

where λ is an eigenvalue.

Neglecting tedious computational details about the linearization and consequent linear stability analysis on the boiling channel, one is directed to the following Section for the comparison of the COMSOL results with RELAP5 and analytical model results.

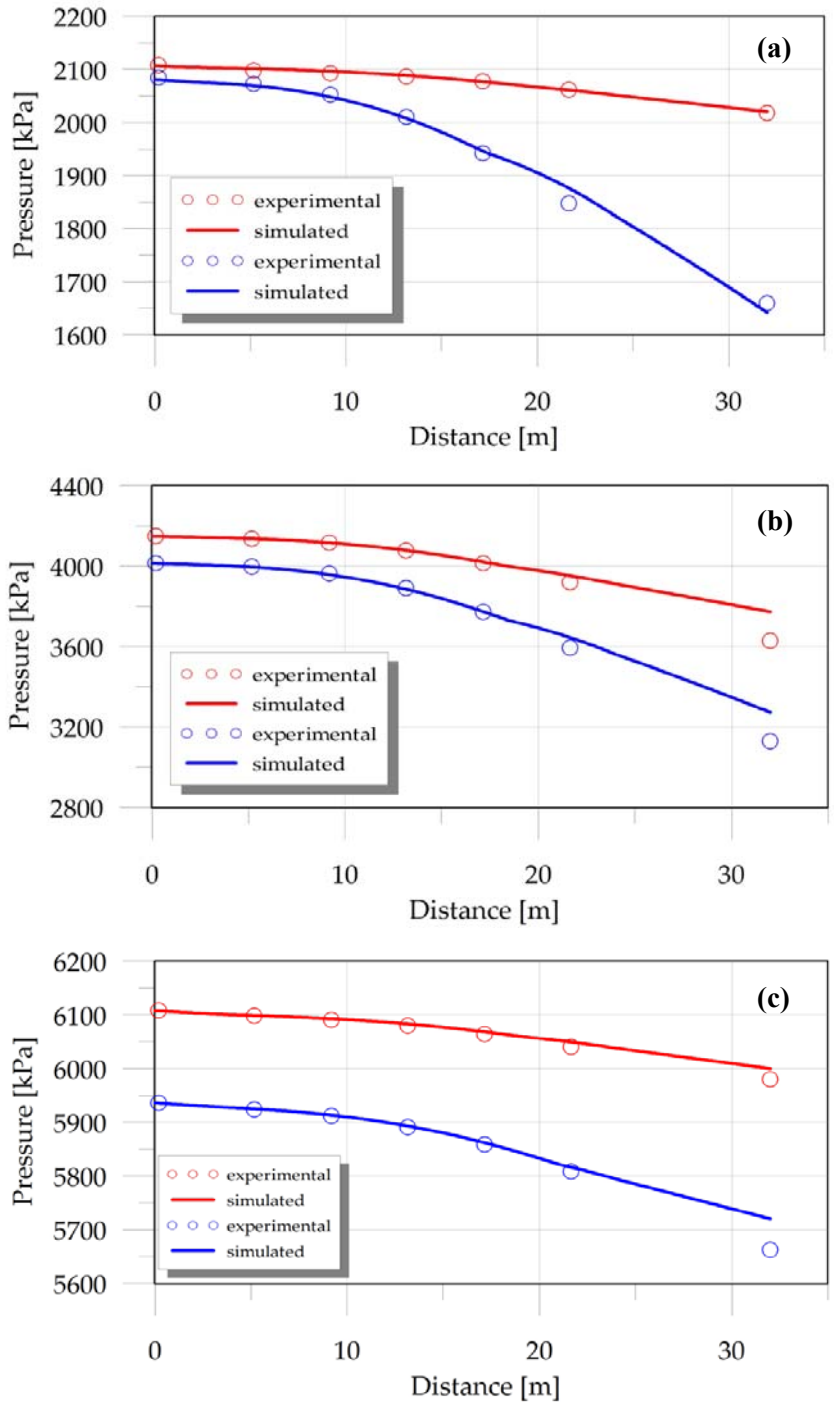

Figure 47 - Comparison of numerical results in COMSOL with Santini's experimental pressure drop data.

(a) - p_{in} = 20 bar – red curve: G = 200 kg/m^{2}s; q" = 43.7 kW/m^2, blue curve: G = 400 kg/m^{2}s; q" = 111.1 kW/m^2.

(b) - p_{in} = 40 bar – red curve: G = 600 kg/m^{2}s; q" = 142.4 kW/m^2, blue curve: G = 800 kg/m^{2}s; q"= 191.6 kW/m^2.

(c) - p_{in} = 60 bar – red curve: G = 400 kg/m^{2}s; q" = 85.2 kW/m^2, blue curve: G = 600 kg/m^{2}s; q" = 117.4 kW/m^2.

6 VALIDATION BENCHMARK OF ANALYTICAL AND NUMERICAL STUDIES ON DWOS

A comprehensive comparison of whole tools developed in this work to predict the inception of DWOs in simple vertical tube geometry is shown in Figure 48, where the noteworthy work of Ambrosini et al. [21] is reported too. Stability maps drawn in the N_{pch}-N_{sub} stability plane are compared. RELAP5 results rely on UVUT model selection, i.e. non-homogeneous non-equilibrium model. Theoretical model uses HEM two-phase flow model, respectively with homogeneous and Friedel friction factor multiplier. Finally, both HEM and DFM are considered as concerns COMSOL results.

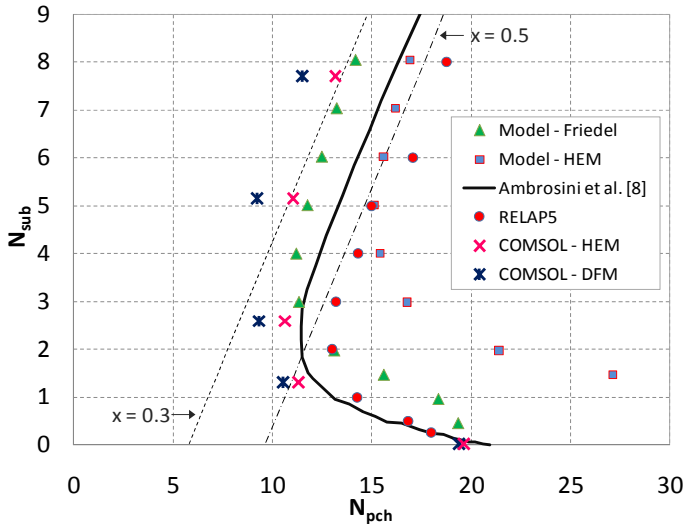

Figure 48 - Validation benchmark between analytical model and numerical models with RELAP5 and COMSOL codes.

It is immediate to notice that all the results with this simple vertical tube geometry confirm the classical DWO theory expectations. The exit quality (proportional to the ratio between thermal power and mass flow rate) turns out as key parameter for the stability boundary definition. At high subcoolings, the stability boundary follows roughly a constant exit quality line; at medium-low subcoolings, the so-named "L shape" appears [23]. On the whole, parametric effect of an increase of the inlet subcooling is stabilizing at high subcooling and destabilizing at low subcooling [3][6].

RELAP5 results found previously an experimental validation, as discussed by Colombo et al. [4]. On this basis, best predictions are offered by the distributed parameter model of Ambrosini et al. [21] and by the proposed two node lumped parameter model with Friedel friction correlation. COMSOL code shows the most unstable region.

However, the applicability of the HEM for calculation of stability threshold is still debatable [38][39]. An alternative to the two fluid approach (complicated by bunch of constitutive relations for interfacial laws) is the DFM, based on a sole momentum equation for the mixture plus non-linear constitutive law for the relative velocity, which should provide more accurate predictions. Nevertheless, it is known that the choice of both concentration parameter and drift-flux velocity significantly affects the stability, since their increase or decrease modifies the void fraction, hence mixture density and transportation time lags [39] [40].

The drift-flux model implemented by COMSOL simulator shows the least agreement, but this discrepancy should be indeed ascribed to the friction factor selected (Jones one, i.e. "high friction" model yielding less stable regions) rather than to the particular DFM parameters adopted.
As the proper prediction of the instability threshold depends highly on the effective frictional characteristics of the reproduced channel (see Section 3.3), the possibility of implementing most various kinds of two-phase flow models (DFM kind, with different void fraction expressions) makes in principle the developed COMSOL model suitable to apply for most different heated channel systems. DFM parameter adjustment will be required separately case by case.

6.1 Main achievements

Before addressing the complex geometry represented by two helical coil tubes for simulation of helically coiled steam generators (Section 7), the developed analytical and numerical modelling tools have been applied to the study of vertical straight geometry (Section 3, 4 and 5), in single and parallel channel configurations. This was mainly due to the difficulties in modelling the influence of helical geometry on instability occurrence and to the small number of appropriate correlations for two-phase friction factor multipliers and void fraction. Besides time domain linear and non-linear studies presented in the previous sections led to understand more in depth the basic phenomena at the basis of DWOs, ranging from development of a self-sustained flow rate oscillation and identification of critical two-phase flow model parameters for accurate prediction of instability threshold, to assessment of experimental apparatus layouts suited for instability detection. State of the art advances reached by the paper results can be summarized as in the followings. Similar discussions have been found in the work of Nayak et al. [39], who investigated various two-phase friction factor multiplier models, DFM parameters and several geometrical parameters in case of two-phase natural circulation system instabilities.

- As concerns the instability mechanism, key role is played by the void propagation time delay in the two-phase region. At sufficiently large values of void fraction (i.e., exit thermodynamic quality), any small fluctuation in the inlet velocity may lead to large fluctuation of the two-phase frictional pressure losses. Multiple feedback effects are triggered by the mandatory constant pressure drop boundary condition. Enthalpy and void transportation lags throughout the channel are evident in a non-sinusoidal wave for flow rate and pressure drop oscillations [12]. "Shark-fin" shape of oscillating total pressure drops is the final outcome.

- When simulating a simple geometry, such as BWR core vertical subchannel, classical DWO theory is respected. Instability boundary shows the "L-shape" inclination in the N_{pch}-N_{sub} plane, with inlet subcooling increase that is stabilizing at high subcooling and destabilizing at low subcooling. The period of oscillations is nearly twice the mixture transit time, and grows with the inlet subcooling.

- Fractional distribution of the pressure drops along the channel plays an important role in determining the stability of the system [12]. In this respect, proper simulation of two-phase frictional pressure losses (prior to proper representation of the pressure drop distribution within the channel) is depicted as most critical concern for accurate prediction of the instability threshold. The homogenous friction factor model shows the most stable

system [39]. Higher friction models (in ascending order: Friedel, Lockhart-Martinelli and Jones) reduce the system stability.

- Two different system layouts are dealt with for instability investigation: a single heated channel (analytically modelled with constant Δp boundary condition, but simulated with RELAP5 according to realistic experimental layout with a parallel bypass to keep the Δp across imposed) and two parallel channels (connected with common headers). The equivalence of the two approaches is found in terms of stability maps, both with analytical calculations (Figure 49: single heated channel is studied with two different values of imposed Δp) and RELAP5 simulations (Figure 41: single heated channel is studied with constant Δp fictitiously impressed and with the bypass nodalization). Such equivalence (strictly valid for the analyzed vertical tube case [6]) is important because, if one has to study the instability boundary of a multi-channel system (i.e., one single channel working rigorously under constant Δp), the experimental apparatus might be designed just with two parallel tubes connected by two headers, thus without the need for a complex parallel large bypass tube.

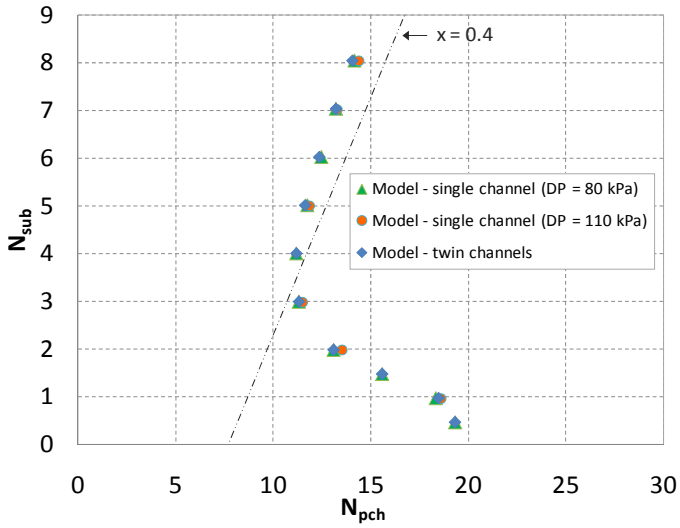

Figure 49 - Stability maps for single heated channel and two parallel channels cases, as calculated with analytical lumped parameter model (Friedel friction model).

- Several sensitivity studies can be provided with the developed models. The effect of tube diameter on boiling channel stability may be relevant when using scaled facilities in simulation of the instability behaviour of prototype systems [39]. Sensitivity analysis with the analytical model (single channel, Friedel friction model), reported in Figure 50, reveals that the stability boundary is independent on tube diameter at high subcooling conditions (where constant exit quality line is roughly respected). On the contrary, the system results less stable as the channel area is reduced at medium-low subcooling conditions. Decrease in tube diameter has destabilizing effect [39], as a reduction of tube area increases the frictional contribution within total pressure drop (but this increase is such to destabilize the system only when the two-phase region is dominant, i.e. at medium-low subcooling).

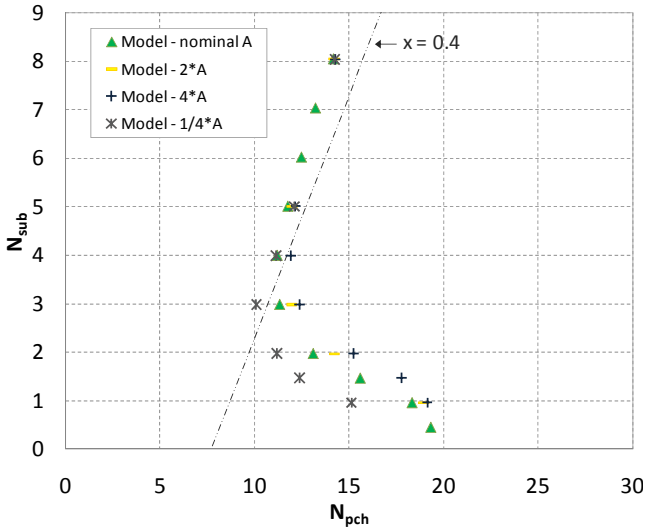

Figure 50 - Effect of channel cross-sectional area on DWO instability threshold, as calculated with analytical lumped parameter model (single channel case, Friedel friction model).

7 COMPARISON BETWEEN MODELS AND EXPERIMENTAL RESULTS

To reproduce and interpret the highlighted phenomena related to the investigated helical coil geometry, both the analytical lumped parameter model and the RELAP5 code have been applied.

7.1 Analytical modelling of the experimental facility

Best results have been obtained via the analytical model, on the basis of a modified form of the widespread and sound Lockhart-Martinelli two-phase friction multiplier, previously tuned on the frictional characteristics of the system [36]. The modified Lockhart-Martinelli multiplier (only-liquid kind) used for the calculations reads:

$$\Phi_l^2 = 1 + \frac{3.2789}{X_{tt}} + \frac{0.3700}{X_{tt}^{2.0822}}. \tag{43}$$

To comply with the form of the modelling equations, passing from "only-liquid" to "liquid-only" mode is required. The following relation [33] is considered:

$$\Phi_{lo}^2 = \Phi_l^2 (1-x)^{1.75}. \tag{44}$$

Though the developed analytical model seems to underestimate the instability threshold conditions (that is, the predicted instabilities occur at lower qualities), rather satisfactory results turn out at low flow rate values (G = 200 kg/m^{2}s). In these conditions, fair agreement is found with the peculiar instability behaviour of helical coil geometry, characterized by a marked destabilization near the saturation when inlet temperature is increased (i.e., inlet subcooling is reduced). Figure 51 shows how the peculiar stability boundary shape, experimentally obtained for the present helical coiled system, is well predicted. Finally, the comparison between model and experimental findings is considerably

better at high pressure (p = 80 bar; Figure 52), where the homogenous two-phase flow model (at the basis of the modelling equations) is more accurate.

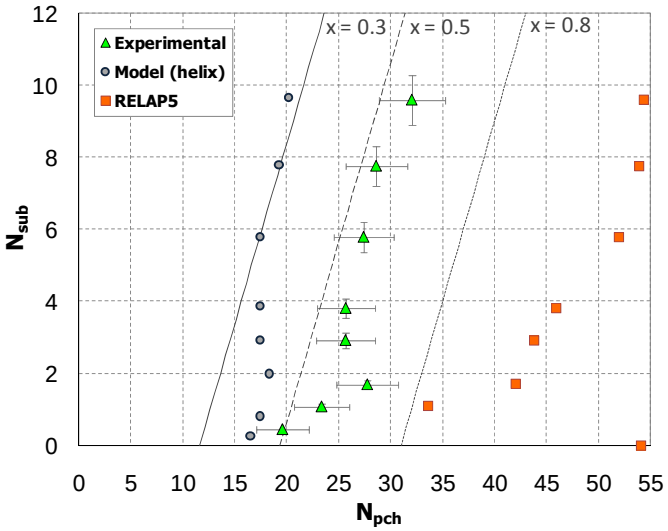

Figure 51 - Comparison between experimental, theoretical and RELAP5 results. p = 40 bar; G = 200 kg/m^{2}s.

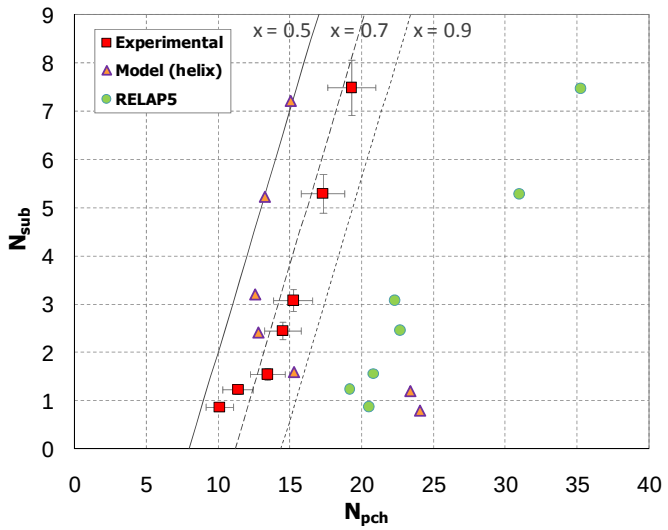

Figure 52 - Comparison between experimental, theoretical and RELAP5 results. p = 80 bar; G = 400 kg/m^{2}s.

7.2 RELAP5 modelling of the experimental facility

Marked overestimations of the instability onset come out when applying the RELAP5 code to the helical coil tube facility simulation (Figure 51 and Figure 52), mainly due to the lack in the code of specific thermo-fluid dynamics models (two-phase pressure drops above all) suited for the complex geometry investigated. More comparison between RELAP5 predictions and experimental data can be found in Figure 53, Figure 54 and Figure 55. The code always depicts a more stable system, consistently with the parametric study of Section 4.2.2, in which a system stabilization was observed increasing the length of the parallel channels. The better predictions are found at pressure p = 40 bar and mass fluxes G = 600 kg/m^{2}s and G = 400 kg/m^{2}s for the lower values of the inlet subcooling. Nevertheless also in these

two cases the code is unable to reproduce the correct threshold behaviour as the system results far more stable at high subcoolings where the instability onset even approaches the iso-quality line at x = 1.0. All things considered, due to the mentioned lack of model implemented in the code to simulate helical geometry, the RELAP5 code cannot be regarded for the time being as a proven tool to study DWO phenomena in helically coiled tubes.

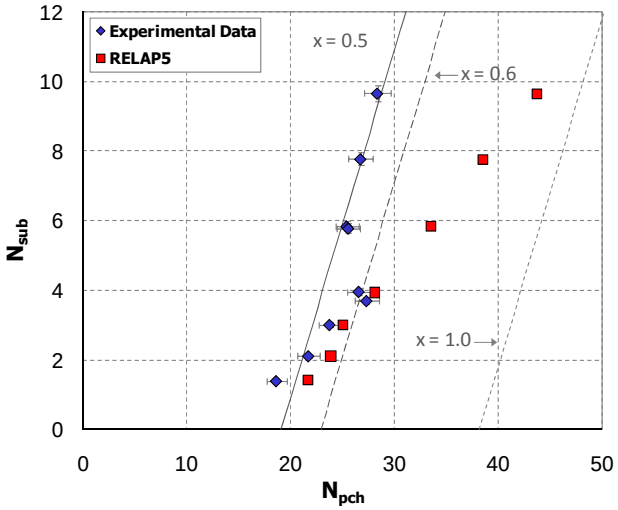

Figure 53 - Comparison between experimental and RELAP5 results. p = 40 bar; G = 600 kg/m^{2}s.

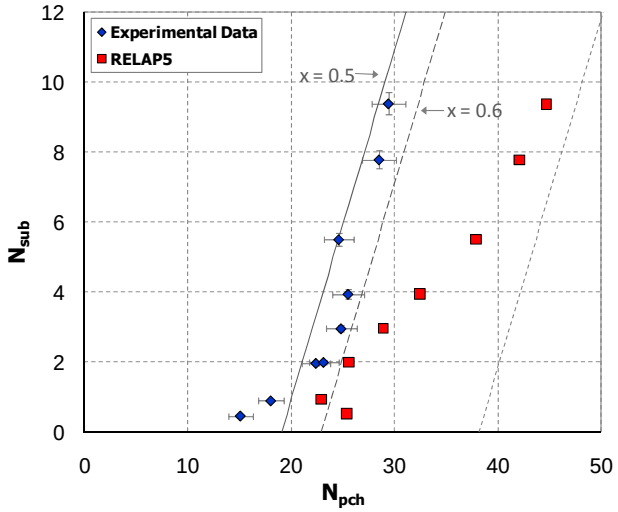

Figure 54 - Comparison between experimental and RELAP5 results. p = 40 bar; G = 400 kg/m^{2}s.

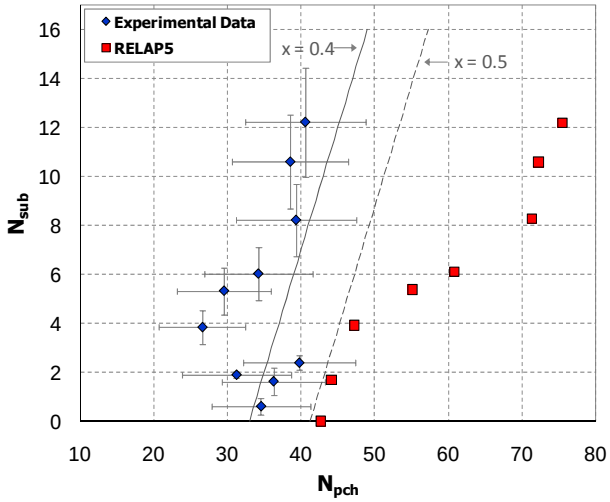

Figure 55 - Comparison between experimental and RELAP5 results. p = 20 bar; G = 200 kg/m^{2}s.

ACRONYMS

BWR	Boiling Water Reactors
DFM	Drift-Flux Model
DWO	Density Wave Oscillation
HEM	Homogeneous Equilibrium Model
IRIS	International Reactor Innovative and Secure
LOCA	Loss Of Coolant Accident
LWR	Light Water Reactor
NASA	National Aeronautics and Space Administration
ODE	Ordinary Differential Equation
PDE	Partial Differential Equation
PDO	Pressure Drop Oscillation
PWR	Pressurized Water Reactor
RELAP	Reactor Excursion and Leak Analysis Program
SG	Steam Generator
SIET	Società Informazioni Esperienze Termoidrauliche
SMR	Small-medium Modular Reactor
UVUT	Unequal Velocity Unequal Temperature

NOMENCLATURE

A	cross sectional area [m^2]
C_0	concentration parameter
c	specific heat [J/kg*°C]
D	diameter [m]
G	mass flux [kg/m^2s]
g	acceleration of gravity [m/s^2]
H	channel height [m]
h	enthalpy [J/kg]
	heat transfer coefficient Eq. (12),(13) [W/m^2*°C]
j	volumetric flux [m/s]
k	valve loss coefficient
L	channel length [m]
M	tube mass [kg]
N_{pch}	phase-change number
N_{sub}	subcooling number
p	pressure [Pa]
q	thermal power [W]
$q"$	thermal flux [W/m^2]

q'''	thermal power per unit volume [W/m^3]
S	slip ratio
	heat transfer surface Eq. (12),(13) [m^2]
T	period of oscillations [s]
	temperature [°C]
t	time [s]
V_{vj}	drift-flux velocity [m/s]
v	specific volume [m^3/kg]
v_c	COMSOL model check variable
X_{tt}	Lockhart-Martinelli parameter
x	quality
w	velocity [m/s]
z	axial coordinate [m]
α	void fraction
λ	system eigenvalue
ρ	density [kg/m^3]
θ	channel inclination angle (with horizontal direction) [deg]
τ	transit time [s]
Φ^2	two-phase friction factor multiplier
Γ	mass flow rate [kg/s]
Ω	characteristic frequency of phase change [1/s]

Subscripts

1φ	single-phase
2φ	two-phase
acc	accelerative
BB	boiling boundary
ex	outlet
fl	fluid bulk
frict	frictional
grav	gravitational
H	homogeneous
h	heated wall
in	inlet
l	liquid
	only-liquid in Eq. (43),(44)
lo	liquid-only
m	mixture
tot	totale
v	vapour

Superscripts

*1*φ	single-phase
*2*φ	two-phase
+	dynamic quality (referred to two-phase density and enthalpy)

REFERENCES

[1] D. Papini, Modelling and experimental investigation of helical coil steam generator for IRIS Small-medium Modular Reactor, PhD Thesis, Politecnico di Milano, Department of Energy, cycle XXIII, Milan, Italy, January 2011.

[2] D. Papini, M. Colombo, A. Cammi, M.E. Ricotti, D. Colorado, M. Greco, G. Tortora, Experimental Characterization of Two-Phase Flow Instability Thresholds in Helically Coiled Parallel Channels, In: Proceedings of International Congress on Advances in Nuclear Power Plants (ICAPP) 2011, Nice, France, May 2-5.

[3] D. Papini, A. Cammi, M. Colombo, M.E. Ricotti, On density wave instability phenomena: modelling and experimental investigation, A. Ahsan (Ed.), Heat Transfer / Book 4, InTech Publisher, Rijeka, 2011, ISBN 978-953-307-584-6.

[4] M. Colombo, A. Cammi, D. Papini, M.E. Ricotti, RELAP5/MOD3.3 Study on Density Wave Instabilities in Single Channel and Two Parallel Channels, *Progress in Nuclear Energy* (submitted).

[5] M. Colombo, A. Cammi, D. Papini, M.E. Ricotti, Numerical Investigation on Boiling Channel Instabilities by Imposing Constant Pressure Drop Boundary Condition via a Large Bypass, In: Proceedings of the International Conference Nuclear Energy for New Europe (NENE) 2010, Portorož, Slovenia, September 6-9.

[6] D. Papini, M. Colombo,. A. Cammi, M.E. Ricotti, Prove sperimentali per canali in parallelo e relative zone di instabilità. Report CIRTEN.

[7] G. Yadigaroglu, Two-Phase Flow Instabilities and Propagation Phenomena, In: J. M. Delhaye, M. Giot, M. L. Riethmuller, (Ed.), Thermohydraulics of two-phase systems for industrial design and nuclear engineering, Hemisphere Publishing Corporation, Washington, 1981, 353-396.

[8] J.A. Bouré, A.E. Bergles, L.S. Tong, Review of Two-Phase Flow Instabilities, *Nuclear Engineering and Design* 25 , 165-192, 1973.

[9] S. Kakaç and B. Bon, A Review of two-phase flow dynamic instabilities in tube boiling systems, *International Journal of Heat and Mass Transfer* 51, 399-433, 2008.

[10] G. Yadigaroglu and A.E. Bergles, Fundamental and Higher-Mode Density Wave Oscillations in Two-Phase Flow, *Journal of Heat Transfer*, Trans. ASME 94, 189-195, 1972.

[11] M.Z. Podowski, Instabilities in Boiling Systems, Third International Topical Meeting on Nuclear Power Plant Thermal Hydraulics and Operations, Seoul, Korea, 1988.

[12] Rizwan-uddin, Physics of Density Wave Oscillations, *International Journal of Multiphase Flow* 20, 4, 721-737, 1994.

[13] M. Ishii and N. Zuber, Thermally Induced Flow Instabilities in Two Phase Mixture, In: Proceedings of the 4th International Heat Transfer Conference, Paris, France, 1970.

[14] M. Ishii, Study of Flow Instability in Two-Phase Mixture, Argonne National Laboratory Report, ANL-76-23, 1976.

[15] P. Saha, M. Ishii, N. Zuber, An Experimental Investigation of the Thermally Induced Flow Oscillations in Two-Phase Systems, *Journal of Heat Transfer*, Trans. ASME 98, 616-622, 1976.

[16] G. Masini, G. Possa, F.A. Tacconi, Flow instability thresholds in parallel heated channels, *Energia Nucleare* 15, 12, 777-786, 1968.

[17] G. Yun, H. Jun, X. Genglei, Z. Heyi, Experiment investigation on two-phase flow instability in a parallel twin-channel system, *Annals of Nuclear Energy* 37, 1281-1289, 2010.

[18] R.T. Lahey Jr., F.J. Moody, The thermal-hydraulics of a boiling water nuclear reactor, American Nuclear Society, USA, 1977.

[19] J.L. Muñoz-Cobo, M.Z. Podowski, S. Chiva, Parallel channel instabilities in boiling water reactor systems: boundary conditions for out of phase oscillations, *Annals of Nuclear Energy* 29, 1891-1917, 2002.

[20] W.R. Schlichting, R.T. Lahey Jr., M.Z. Podowski, An analysis of interacting instability modes, in a phase change system, *Nuclear Engineering and Design* 240, 3178-3201, 2010.

[21] W. Ambrosini, P. Di Marco, J.C. Ferreri, Linear and Nonlinear Analysis of Density Wave Instability Phenomena, *International Journal of Heat and Technology* 18, 1, 27-36, 2000.

[22] G. Yun, S.Z. Qiu, G.H. Su, D.N. Jia, Theoretical investigations on two-phase flow instability in parallel multichannel system, *Annals of Nuclear Energy* 35, 665-676, 2008.

[23] Y.J. Zhang, G.H. Su, X.B. Yang, S.Z. Qiu, Theoretical research on two-phase flow instability in parallel channels, *Nuclear Engineering and Design* 239, 1294-1303, 2009.

[24] US NRC Nuclear Safety Analysis Division, RELAP5/MOD3.3 Code Manual, NUREG/CR-5535/Rev 1, 2001.

[25] W. Ambrosini, J.C. Ferreri, Analysis of Basic Phenomena in Boiling Channel Instabilities with Different Flow Models and Numerical Schemes, In: Proceedings of 14th International Conference on Nuclear Engineering (ICONE 14), Miami, Florida, USA, July 17-20, 2006

[26] COMSOL, Inc., COMSOL Multiphysics® User's Guide, Version 3.5a, 2008.

[27] W.R. Schlichting, R.T. Lahey Jr., M.Z. Podowski, M.Z., T.A. Ortega Gómez, Stability analysis of a boiling loop in space, In: Proceedings of the COMSOL Conference 2007, Boston, Massachusetts, USA, October 4-6.

[28] L. Santini, A. Cioncolini, C. Lombardi, M.E. Ricotti, Two Phase Pressure Drops in a Helically Coiled Steam Generator, *International Journal of Heat and Mass Transfer* 51, 4926-4939, 2008.

[29] M.D. Carelli, L.E. Conway, L. Oriani, B. Petrović, C.V. Lombardi, M.E. Ricotti, A.C.O. Barroso, J.M. Collado, L. Cinotti, N.E. Todreas, D. Grgić, M.M. Moraes, R.D. Boroughs, H. Ninokata, D.T. Ingersoll, F. Oriolo, The Design and the Safety Features of the IRIS Reactor, *Nuclear Engineering and Design* 230, 151-167, 2004.

[30] L. Santini, D. Papini, M.E. Ricotti, Experimental Characterization of a Passive Emergency Heat Removal System for a Gen III+ Reactor, *Science and Technology of Nuclear Installations* 2010, doi: 10.1155/2010/864709, 2010.

[31] R.J. Moffat, Describing the Uncertainties in Experimental Results, *Experimental Thermal and Fluid Science* 1, 3-17, 1988.

[32] The Math Works, Inc., SIMULINK® software, 2005.

[33] N.E. Todreas, M.S. Kazimi, Nuclear Systems I: Thermal Hydraulic Fundamentals, Taylor and Francis, Washington, DC, USA, 1993.

[34] D. Papini, Modeling and Experimental Investigation of Two-Phase Flow Instabilities in Helically Coiled Steam Generator Tubes, In: 5th ENEN PhD Event 2011, International Congress on Advances in Nuclear Power Plants (ICAPP), Nice, France, May 4, 2011.

[35] G. Giorgi, Single and parallel channel stability analysis by means of multi-physics modeling, MSc Thesis, Politecnico di Milano, Department of Energy, Milan, Italy, October 2010.

[36] D. Colorado, D. Papini, J.A. Hernández, L. Santini, M.E. Ricotti, Development and experimental validation of a computational model for a helically coiled steam generator, *International Journal of Thermal Sciences* 50, 569–580, 2011.

[37] L. Santini, Thermalhydraulic issues of IRIS nuclear reactor helically coiled Steam Generator and Emergency Heat Removal System, PhD Thesis, Politecnico di Milano, Department of Energy, cycle XX, Milan, Italy, 2008.

[38] N. Goswami, S. Paruya, Advances on the research on nonlinear phenomena in boiling natural circulation loop, *Progress in Nuclear Energy* 53, 673-697,2011.

[39] A.K. Nayak, P. Dubey, D.N. Chavan, P.K. Vijayan, Study on the stability behaviour of two-phase natural circulation systems using a four-equation drift flux model, *Nuclear Engineering and Design* 237, 386–398, 2007.

[40] Rizwan-uddin, J.J. Dorning, Some nonlinear dynamics of a heated channel, *Nuclear Engineering and Design* 93, 1–14, 1986.